

TECHNOLOGY FOR RESTARTING MOLTEN SALT NUCLEAR FUEL CHEMISTRY AT MU

A Thesis

presented to

the Faculty of the Graduate School

at the University of Missouri-Columbia

In Partial Fulfillment

of the Requirements for the Degree

Master of Science

by

ERIC A. SCHWARZ

Dr. Patrick J. Pinhero, Thesis Supervisor

MAY 2011

The undersigned, appointed by the dean of the Graduate School, have examined the thesis entitled

TECHNOLOGY FOR RESTARTING MOLTEN SALT NUCLEAR FUEL CHEMISTRY AT MU

presented by Eric A. Schwarz,

a candidate for the degree of Master of Science, and hereby certify that, in their opinion, it is worthy of acceptance.

Professor Patrick J. Pinhero

Professor John Gahl

Professor Paul Chan

ACKNOWLEDGEMENTS

I would like to thank Professor Patrick J. Pinhero for keeping my attention to my work when I lacked the courage to do so.

I would like to thank the Government of the United States of America for the financial support for my project and the countless experts in the field over the last six decades that have truly pioneered this art. It also includes the US Nuclear Regulatory Commission (USNRC) for funding to support my stipend and project and the US Department of Energy which has granted equipment through the ERLE program. It has made the restart of this program possible and its future bright.

I should also thank Recycled Chemicals, a division of Environmental Health and Safety (EHS) at MU for providing a large amount of unused chemicals at no-cost as I experiment and explore which saved thousands of dollars in glassware and chemicals.

Many thanks to the people of the University of Missouri Research Reactor (MURR) for analytical work using nuclear techniques, especially Dr. Mike Glascock for his generous advice and analytical experience.

For the use of Atomic Force Microscopy, I am indebted to Kevin Zurick for his help getting the images and to Zack Thacker for the Auger Electron Microscopy images and elemental data.

Table of Contents

List of Figures.....	iv
List of Tables.....	v
Chapter 1 Introduction.....	2
Chapter 2 Literature Review.....	5
2.1 Electrochemical Principles.....	5
2.2 Molten Salt Chemistry.....	11
Chapter 3 Experimental.....	15
3.1 Materials and Equipment.....	15
3.2 Chemical Reactor Equipment.....	20
3.2.1 Electrochemical Reactor Vessel.....	20
3.2.2 Counter and Working Electrodes.....	21
3.2.3 Reference Electrode.....	21
3.2.4 Electrochemical Cell System.....	25
3.3 Sample Preparation.....	26
3.4 Analytical Methods.....	26
Chapter 4 Results and Discussion.....	28
4.1 Reference Electrode performance and characterization.....	28
4.2 Cerium Deposition onto Tungsten.....	41
4.3 Electrochemical examination of Green Mill Tailings from Southeastern Missouri.....	45
Chapter 5 Conclusions.....	46
References.....	47
Appendix: Laboratory Molten Salt Procedures.....	52

List of Figures

Figure 1. Structure of tributyl phosphate (TBP), demonstrating the large butyl substituents.	3
Figure 2: Purification Scheme for argon gas cleaning.	18
Figure 3: Simplified Reference Electrode in use at MU Chemical Engineering.	24
Figure 4: Electrochemical Cell Electrode Assembly.....	25
Figure 5. (a) Sample A, (b) Sample B, (c) Sample C and (d) is a blank (containing no Ce added).....	29
Figure 6. Plot of current magnitude as a function of the scan rate.	31
Figure 7. Standard deviation in the current signal (between Samples A, B and C) as a function of applied potential using the MMSSC RE.	32
Figure 8. Standard deviation in the current signal (between Samples A, B and C) as a function of applied potential using the Pt QRE.....	33
Figure 9. Bode plot of 500 ppm Ce with Th turnings added following anodic dissolution.	36
Figure 10. Nyquist plot of 500 ppm Ce with Th turnings added following anodic dissolution.	37
Figure 11. XRF results on sectioned mullite samples CER003, CER004.	38
Figure 12. Concentration of various elements for samples CER005, CER006 (virgin mullite) from NAA.	39
Figure 13. DPV on Sample F (Ce solution in LiCl-KCl) showing the Ce(III) to Ce(0) peak.....	42
Figure 14. Chronocoulometry run for Sample F to extract Ce metal from melt.....	42
Figure 15. Tungsten foil blank.	43
Figure 16. Tungsten foil after Ce deposition and salt immersion.	44

List of Tables

Table 1. Breakdown of Relevant Techniques and Data Collected for Electrochemical Work.....	5
Table 2. Important aspects when utilizing the Cottrell equation.	8
Table 3. Relative magnitude of current as a function of pulse height and electrons involved in the reaction. ⁴	11
Table 4. Concentration Data and uncertainty for each sample.	28
Table 5. Current magnitudes for each sample as a function of scan rate.....	30
Table 6. CER006 elemental composition and uncertainty in descending concentration.	40
Table 7. Concentration-weighted polarizabilities in mullite (Sample CER007).....	41

Chapter 1 Introduction

Recycling of Used Nuclear Fuel (UNF) has the benefits of reducing the mass and volume of radioactive or nuclear material stored in a monitored, retrievable location, as defined by the Nuclear Waste Policy Act of 1980 (NWP) (and, as amended in 1982) as well as preventing the diversion of materials-of-interest to terrorist groups by securing it in the safest place possible: another fuel assembly loaded into a nuclear reactor core. Reprocessing fuel is an act of recycling whereby the 'unburned' fuel is separated from the used material, transuranics (TRU) and fission products, and the unused components are remade into new fuel.

Nuclear and chemical engineering research¹ over the last two decades has seen an increase in the technology known as 'pyrochemical reprocessing', or 'molten salt reprocessing', or 'non-aqueous reprocessing' or 'dry reprocessing'. Each of these terms is, in general, interchangeable and for the scope of this work they are considered equivalent. Here, the focus is use of molten alkali-halide salt—a lithium chloride-potassium chloride (eutectic) mixture, as a solvent/ electrolyte in an electrochemical extraction process when the proper electrode potentials are applied. For the process of electrochemical partitioning to be efficient and economical, basic science concerning the process at the laboratory scale must be improved. The work here is the beginning of MU Chemical Engineering restarting molten salt science and technology research.

Molten Salts used in reprocessing of nuclear fuel have many advantages over traditional aqueous methods. The most prominent aspect of nuclear fuel recycling is the radiological hazard associated with its handling. While most reprocessing technologies attempt to reduce this hazard by allowing for the shorter-lived radionuclides to decay and typically these species contribute to a large beta and gamma source, there are some long-lives species that decay by intense (high-energy) gamma

and beta modes. Therefore, even if the majority is allowed to decay, this does not solve the entire problem. Although this higher-intensity radiation presents an operational personnel hazard, it also degrades the solvents used in the aqueous process. That is, this intense, ionizing radiation begins to fragment molecules: a process called 'radiolytic decomposition'. This radiolytic decay is responsible for all types of operational issues at commercial and other nuclear power plants since the chemical used to maintain reactivity or corrosion control become fragmented. It is not too difficult to imagine this same degradation, but now on a wider and more problematic scale, with much larger and 'floppier' organic molecules, such as tributyl phosphate (TBP)—the traditional actinide separation organic phase.

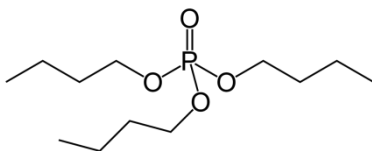


Figure 1. Structure of tributyl phosphate (TBP), demonstrating the large butyl substituents.

In order to create a useful organic phase separation in aqueous solution, the molecule must exhibit both hydrophilic and hydrophobic characteristics, as TBP does here. Research into various other molecules of similar structure have not yielded separation efficiencies that make them more attractive, especially if a requirement for the molecule is that it be resistant to radiolytic decomposition.

Radiolytic decomposition presents a serious engineering and safety problem as the decomposition products can be flammable, explosive or reactive.² Such compounds can include methane and hydrogen gas which must be dealt with in the process, especially if the fuels undergoing separation are radiologically hot. However, as mentioned above, some nuclides which are fission products such as cesium-137, have half-lives that span on the order of years to tens of years. But fission products

are not the only source of longer-lived nuclides. Nuclear fuel is manufactured with cladding and is exposed to a high neutron flux during its service lifetime. The cladding can be stainless-steel, aluminum or in the case of commercial reactor cladding, Zircaloy. This alloy is a mixture of zirconium, tin, iron, chromium and hafnium. While the zirconium exhibits an excellent neutron-transparent characteristic, it too can become activated or undergo a neutron capture reaction, making it radioactive. There are several isotopes of natural iron and, as a result, subsequent neutron captures will usually undergo no radioactive decay. However, if enough Fe-58 is present, this may activate and decay to cobalt-59 which has a large neutron cross section for neutron capture. This will lead to the production of Co-60 which has a half-life of 5.25 years and gives off two, high-energy gamma photons for its decay.

Chapter 2 Literature Review

2.1 Electrochemical Principles

Solute concentrations are difficult to work with $<10^{-4}$ M because the solvent and the supporting electrolyte are the same entity.³ This sets the lower operation bound to approximately 10 ppm Ce. It is noteworthy to express that the LiCl-KCl that comes premixed (Sigma-Aldrich, 44-wt% LiCl-KCl eutectic beads) as the eutectic and it contains many impurities that exceed this concentration threshold. An upper limit on concentration of the analyte can also be imposed to maintain the activity coefficients close to unity. This upper limit corresponds to mole fraction of 0.01, or for cerium this is approximately 25,000 ppm. Therefore, if concentration is kept below this value, we can consider these solutions 'dilute' and the calculations that require activity can be directly computed through knowledge of the concentrations.³ Table 1 displays an overview of the different electrochemical techniques applied to molten salt analysis.

Table 1. Breakdown of Relevant Techniques and Data Collected for Electrochemical Work

Technique	Input Required	Output Measured	Resulting Information
Potentiometry/ Open-Circuit Potential	Temperature, concentrations or standard potential	Potential difference between electrodes	emf, Gibbs and excess free energy; stability
Voltammetry	Potential	Current as function of potential	Diffusion data, concentration
Chronoamperometry	Large potential step to mass-transfer limit region	Current as a function of time	Diffusion coefficient, stability of species
Controlled-Potential Coulometry	Stable potential	Current as a function of time to give charge	Current can be related to diffusion (may or may not be useful with stationary electrodes)
Controlled-Current Coulometry	Stable current	Potential as a function of time	Concentration; kinetics
Differential Pulse Voltammetry	Temperature, Pulse Amplitude	Current, Differential Current vs. Potential	Improved detection limits; improved identification; Differential current removes background and charging current from data

Potentiometry or Open-Circuit Potential (OCP) is used to measure emf and the Gibbs and excess free-energies and to study the stabilities of several compounds. A reduced species (R) is in equilibrium with its oxidized species (O) according to the reaction



where n is the number of electrons transferred in a transition between the two species.

Application of the Nernst equation

$$E = E^0 + \frac{RT}{nF} \ln \left(\frac{a_O}{a_R} \right) \quad (2)$$

which demonstrates the relationship of a measured potential (E) to its standard potential (E^0) due to the natural log of the solute's oxidized and reduced activity ratio (a_O/a_R) with R the ideal gas constant, T is the temperature and F is Faraday's constant which is the total charge of one mole of electrons (given as $96,485 \text{ C mol}^{-1}$). The activity is the ionic 'effect' of the charged species in the solution as is related to its concentration, c , using an activity coefficient, γ , as shown in the following equation for the i -th species.

$$a_i = \gamma_i c_i \quad (1)$$

Usually, however, using a reference electrode with the concentration between the lower and upper bounds one can now use the Nernst equation as

$$E_{cell} = E^0 + \frac{RT}{nF} \ln \left(\frac{C_O}{C_R} \right) + E_j \quad (2)$$

where E_j is the junction potential of the cell, and for molten salt systems is usually negligible.³

Linear Sweep Voltammetry (LSV)/ Cyclic Voltammetry (CV) are two procedures that observe a change in working electrode (WE) current as a function of the applied potential to the WE. As the names suggest, CV is just LSV which sweeps a previous set of potentials in the opposite direction. This method is rapid and somewhat repeatable, especially in reversible systems. Redox peaks, as they are often called behave more as 'waves' in these voltammograms since they exhibit a more gentle rise and fall. The difficulty in using these voltammograms is that the current noise can conceal some features even with fast scan rates.

Chronoamperometry (CHA) is the application of a large amplitude potential step and measures the current response from that perturbation. This is accomplished by controlling the working electrode's potential from a point of no reaction to a potential that enables electrolysis. The goal is to have the potential step so large that the reaction is instantaneously mass-transfer limited. This means that the current decays as a factor of $t^{-1/2}$, or inversely-proportional to the square root of time. The Cottrell equation can show the relationship of some fundamental parameters **for a reversible reaction**. This Cottrell equation is

$$i = nFAC_O^* \sqrt{\frac{D_O}{\pi t}} \quad (3)$$

and A is the surface area of the electrode (in cm^2), C_O^* is the initial bulk molar concentration (mol cm^{-3}) and D_O is the diffusion coefficient. The subscript denotes for the oxidized species. This equation is valid for round or square electrode surfaces, such as tungsten disk employed in the present molten salt electrochemical study.⁴ The other values are as defined earlier. This also demonstrates the control that diffusion has over electrolytic operations.

Table 2. Important aspects when utilizing the Cottrell equation.

Excessive Current <ul style="list-style-type: none">• Large current pulses at $t \approx 0$.• Instrumentation limits data output.
Instrumentation Limitation <ul style="list-style-type: none">• Recording instrumentation may be saturated due to a current overload that may prevent seeing early features in the data.
Nonfaradaic Charging <ul style="list-style-type: none">• During these large potential steps, there is a nonfaradaic current that flows and as a result the R_u (uncompensated resistance) and C_d (double-layer capacitance) produce a cell time constant at which the cell's current decays.
Convection Effects <ul style="list-style-type: none">• The diffusion layer may be affected by outside vibrations or from large density gradients formed during long electrolysis and this will tend to produce currents that are larger than that expected from the Cottrell equation.

A double-potential step method can be used to examine the stability of species formed by electrochemical analysis. Therefore, it has more applicability for quasi-reversible reactions and does not seem suited for completely-reversible reactions.³

With respect to nonfaradaic charging, as mentioned above, this effect is a result of current that is used to charge the electrode double layer capacitance (C_d). This phenomenon is, obviously, an artifact whose duration can be computed, as in the well-known capacitor charging relationship

$$i_{nf}(t) = \frac{V_0}{R_u} e^{-\frac{t}{\tau_0}} \quad (4)$$

where i_{nf} is the non-faradaic current, V_0 is the initial voltage at $t = 0$, R_u is the uncompensated resistance of the electrode double layer, τ_0 is the characteristic time constant which is equal to $R_u C_d$.

This will only have an appreciable effect in five time constants and afterward there is no further participation. Bard and Faulkner state⁴ that to assume a completely instantaneous change at $t = 0$, the data collection time must be larger than that of $R_u C_d$. Using AC methods, especially EIS, one can determine the value of the time constant.

Controlled-Potential Coulometry (CPC) is the best method for determining the number of electrons involved in a redox reaction³. By knowing a few parameters, one can easily calculate for the number of electrons involved in the electrochemical reduction, n . The most efficient method of conducting an electrolytic operation is with a controlled potential since the current is always a maximum and is consistently maintained at or as close to a 100% current efficiency as practicable.⁴

The total charge (Q_{total}) passed during the reaction can be measured easily with modern instrumentation. This is the total coulombs passed over a known time, as in

$$Q_{total} = \int_0^{\infty} i(t) dt \quad (5)$$

where Q is the number of coulombs, $i(t)$ is the current during the CPC.

The electrode reaction must satisfy the following basic requirements, however:

1. It must be of known stoichiometry,
2. it must be a single reaction (or at least no other side reactions of different stoichiometry),
and
3. it must occur as close to 100% current efficiency.

As $t \rightarrow \infty$, this indicates the extent of the electrolysis and Equation 1 can be solved above as

$$Q_{total} = \int_0^{\infty} i(t) dt = nFN_O = nFVC_O^* \quad (6)$$

where N_O is the initial moles of the oxidized species, V is the solution volume (in cm^3) and C_O^* is the initial bulk molar concentration (in mol/cm^3). Also, n and F have again the same meanings.

The number of electrons, n , involved in the reaction can be determined without prior knowledge of the diffusion coefficient or the electrode surface area whereas voltammetric methods must necessarily know the diffusion coefficient and the electrode area as well as the reversibility of the reaction *a priori*.

Differential Pulse Voltammetry (DPV) examines the chemical system with a response of differential current caused by the perturbations of a slowly changing applied potential along with a short-duration pulse applied over the existing potential. Usually, this is also referred to as Differential Pulse Polarography, although polarography is more commonly associated with the use of a Dropping Mercury Electrode (DME) as the WE. Here, DPV can be employed for molten salt systems as well as any solid electrode, contrary to polarography. In fact, detection limits for electrochemical systems exhibit a substantial improvement (10^{-6} M or better is observed in some systems).⁴ Perhaps the greatest benefit is that a differential current is the output parameter. This effectively cancels the background and charging current which are artifacts of the high temperatures and large conductivities not usually associated with aqueous systems but are encountered in molten salt systems. One of the main aspects is that when a potential is sufficiently negative to restrict the system to the mass-transport limited region, there will be no change in current and therefore only the region with the largest differential current will show as a peak at the reduction potential for the given system.

Table 3. Relative magnitude of current as a function of pulse height and electrons involved in the reaction.⁴

Pulse Height (mV)	<i>n</i> =1	<i>n</i> =2	<i>n</i> =3
-10	0.0971	0.193	0.285
-50	0.453	0.750	0.899
-100	0.750	0.960	0.995
-150	0.899	0.995	-
-200	0.995	-	-

2.2 Molten Salt Chemistry

Electrorefining metals from salts is not new. This method for creating a pure metallic product is quite simple and has been commercially employed for at least a century with good efficiency. However, electrorefining of uranium might be considered more technologically-important since it occurs before uranium metal was required as a nuclear fuel. Engineers at Westinghouse developed a process in 1932 for the extraction of pure uranium metal from a molten salt.⁵

The Manhattan Project however, required large amounts of metal for metallurgical study at first and then even larger amounts for weapons and reactor fuels.⁶ From previous experience, we knew that the uranium metal was too reactive to be handled in air and use of an aqueous process had some difficulties since a chemical process is needed to convert the purified oxide to the desired form. Usually, this involved fluorination since, as a gas, the natural uranium is enriched in ²³⁵U. Ames Lab at the Iowa State University was dedicated to recovering large amounts of uranium and thorium metal from ores and developing efficient methods for future work.⁷ Their technique was simple: thermophysical bomb reduction of thorium fluoride. By melting a reductant (e.g. lithium metal)

along with the salt of the oxide of interest in a sealed container, the appropriate redox reaction consumed the reductant and left the base uranium or thorium metal behind.

The Experimental Breeder Reactor (EBR-I)⁸ at the Idaho National Laboratory became the next logical technological step in molten salt chemistry work. This reactor plant design was to demonstrate the engineering feasibility of generating both electricity and fuel simultaneously. Theoretically, it was also said that EBR-I could possibly generate more fuel than it consumed in the process, which is a major technological breakthrough for humanity as no other power generation process ever comes close.

The essential design used is a 'blanket' of 'fertile' material (²³⁸U or ²³²Th) which surrounding the core or 'seed', which is the reactor's driver fuel. The seed is highly-enriched ²³⁵U. This resulted in significantly large reactivity for long core operation and excess neutron production. With a large positive fuel reactivity, plenty of fertile material could be loaded without significantly affecting the core criticality during burnup. The surrounding blanket receives a substantial neutron flux, moderated to the right energy, to make the capture reaction efficient. After approximately 30 days, some of the fertile material was converted or 'bred' into ²³⁹Pu, using the following nuclear reactions of Equations 7 – 9.



A chemical separation process to remove the newly-generated fuel from the blanket material has to be performed since the U²³⁸ was converted or transmuted to a different chemical element altogether (Pu²³⁹). In addition to the fuel that is present, other products can develop. These are

known collectively as the 'minor actinides' (MA) because they are present in such small quantities. However they are generated by subsequent neutron capture and beta-minus decay, thus driving the proton or atomic number higher until this is no longer efficient. Typical MAs include Am, Cm along with some Cf and Bk. The latter two are usually negligible. Studies to separate these were also undertaken since these elements make up a large portion of the radioactivity and decay heat of UNF and also have other technological uses (e.g. Am²⁴¹ is used in smoke detectors and Cf²⁵² is a portable neutron source).^{9,10,11,12}

Chemical separation is accomplished either through an aqueous or non-aqueous method. The aqueous method was developed and refined over the last several decades, from the strategic weapons program which required large plant operations operating for approximately 30 years in the United States. The aqueous process is straight-forward: dissolve the material, use an organic solvent to perform a liquid-liquid extraction by the chemical environment and recover the material. Liquid-liquid extraction takes advantage of the hydrophilicity or hydrophobicity of a chelated metal's ligands to migrate to one of the immiscible layers and remain there.

In the late 1940's and early 1950's at the Hanford Atomic Products Operation (HAPO) (though known by various names from various contractors, which is now the site of Pacific Northwest National Laboratory (PNNL)) in Hanford, Washington, a second method was explored for actinide separation. Some of the early researchers and engineers began to look at these alternatives and it seems that this is where the ideas for nuclear fuel reprocessing with molten salts started. Other researchers also explored the usefulness of these molten salt reprocessing techniques.^{13,14,15,16,17,18}

Later work focused on extraction and purification of large quantities of plutonium metal, especially using different techniques, at Los Alamos National Laboratory.^{19,20,21,22} The work there was

principally geared toward better production scale equipment for kg-sized quantities. Even studies concerning processes that could be continuous, as opposed to batch, were examined.²³

By the end of the 1970's, however, there was a shift in policy²⁴ concerning nuclear fuel processing. People became concerned with the wastes generated as well as the possibility of diversion of plutonium to terrorists. The nuclear weapons production industry had, by this time, been severely cut back but all of the knowledge and experience regarding chemical processing of the actinides had matured^{25, 26} considerably. Indeed, new directions²⁷ for molten salt work were even being explored to create symbiotic fission-fusion reactors as a potential evolutionary step.

The University of Missouri (MU) got involved in a program during the 1990's to study the fuel separations from UNF using a molten LiCl-KCl salt, led by Prof. Truman "Turk" Storvick here in the Department of Chemical Engineering. This collaborative program was between MU and Rockwell international (before being acquired by Boeing). This program was called TRUMP-S (TRansUranic Molten salt Pyropartitioning-Separation) and it studied, in part, the thermodynamics of actinide separations using Am and Pu obtained from the US DOE.^{28,29} This project also examined the separation of the lanthanides from the actinides, since these two groups have very similar reduction potentials.³⁰ Later work focused on system design of the cathode to improve separations.³¹

At about this same time, Argonne-West began examining methods for disposal of the EBR-II (2nd generation of the EBR) since it contained metallic uranium (highly-enriched) sodium-bonded fuel elements.³² Since such a large amount of material was present, a larger-scale system for recovery was needed.

Further work has been steady over the years since the 1990's. In Europe, Japan and Korea, many groups continue to investigate and gather important information to make molten salt electrochemical separations more feasible for UNF applications.^{33,34,35}

Chapter 3 Experimental

3.1 Materials and Equipment

For the work of molten salt electrochemistry, the materials options for use are usually limited to two major criteria: corrosion resistance (particularly that of the chloride corrosion) and heat resistance. Other factors that may influence the materials include resilience during heatup and cooldown (not too significant for small systems but still somewhat important) and porosity. For example, most equipment in use should be nonporous as the porosity would allow for molten salt to become trapped within these pores or gaps and then create problems on freezing or melting.

Quartz has been a popular material for many decades and with good reason: it is a glass that is quite resistant (though not completely) to halide corrosion as well as a good high-temperature resistor in molten salt. Early work carried out here employed quartz tubing as sheaths for platinum electrodes as these added non-conductive rigidity to the electrodes. But quartz does breakdown eventually and must be replaced. Visible etching is evinced early on with only a few days work even in a dry environment.

Ultimately, to perform molten salt chemistry, an inert atmosphere must be maintained. This has two major requirements: 1) outside moisture must be prevented from entry and, 2) any moisture that does enter the system should be removed. Therefore, to achieve these criteria, a system to promote boundary system integrity is employed in tandem with an atmospheric purification system.

Here, a 77-cu. ft. (2200 L) stainless-steel glove box is utilized to create a working volume or containment which is robust enough to handle most operations regarding molten salt chemistry. The operator then interacts with the sample using gloves made from Buna-N material. This is ideal

since, although it is not particularly as chloride corrosion-resistant as fluorinated polymers, it does offer substantial resistance in low-concentration environments and is very cost-effective.

Introduction of materials into the box must be accomplished and this is done by both engineering and procedural controls. Two antechambers (buffer zones) are available (one large and one small) to permit transfer of equipment and materials. These are, by procedure, 'rinsed' or flushed with argon gas (of operating box quality) through six cycles of evacuating (to $\sim 10^{-2}$ Torr) and then refilling (to about -10 mmHg gauge as there is no need to equalize until the last filling before entry).

An obvious feature or requirement of gloveboxes is that they must remain essentially leak-free. The definition of leak-free could mean different things to different people and different uses of glove boxes but here it is defined as having a known leak rate of less than 2×10^{-8} atm-cc/ s. For this to be achievable, a He mass-spectrometer leak-detector is employed. Usually there is a calibrated leak that can be used to convert He leakage to air leakage but this is seen as unnecessary. Since the glovebox and the outside surroundings are at, essentially at 1 atm of pressure, the leak rate maximum limit is simply 20 pL/ s. Leaks, while troublesome because of the loss of pure inerting gas (which is not without cost), create a problem with the back diffusion of moisture and oxygen into the box.³⁶ While moisture can create corrosive gases, the oxygen will readily oxidize electropositive metals (e.g. lanthanides and actinides) creating insoluble oxides which will reduce separation efficiency. This is certainly the major issue at play. However, in the employment of glove boxes for actinide chemistry research, the containment boundary also acts to keep alpha-emitting constituents within the box and the leak-tightness of the box plays a more critical role.³⁷ Leak tightness must also be achieved in parts of the system that are not necessarily gaskets and seals on the box but also support equipment and that which transfers gas to and from the support equipment: hoses. The hoses used are a vinyl tubing with nylon reinforcing 'spiral' which is fastened

to KF-40 (QF-40) flanges using a hose-clamp. The technique required for these hose clamps is extraordinary: to make a completely gas-tight seal, the hose should have the flange sunk all the way in but rather halfway to give sufficient purchase on the flange but not allow for any deformity (that may be caused by the hose running up the edge of the flange). Also, the hose clamp should be plumb against the edge of the hose to prohibit flaring of the extra hose material. This is a prime source of leaks and should be examined immediately for leaks.

A He leak detector is only as good as its employment: the locations must be found and the instrument must be used properly and consistently. Once a calibration check on the leak detector is performed, the glovebox is evacuated (to no more than ± 5 "H₂O gauge to prevent damage to gloves) and then backfilled with He gas a few times (5 times is sufficient) to give a large He presence in the atmosphere due to its highly diffusive nature within the containment, regardless of the elevation within (since He is quite light compared to Ar, one might expect for only the high points to have 'visible' leaks but this is not the case: He is sufficiently filling in the whole space and the sensitivity of the instrument can detect very low concentrations of He gas).

For these studies, the atmosphere was maintained at high-purity as a result of two factors, the makeup gas purity was kept low and the operating gas was purified. A makeup gas manifold was constructed to permit swapping of argon bottles online without interruption which permits a redundant supply of gas in case of a loss of the primary source. Immediately downstream is a molecular sieves drying column to strip out any remaining moisture from the gas before injection in to the box. While industrial grade argon gas is usually on the order of 10 ppm moisture, these sieves further clean the gas down to <1 ppm and allows for a less-expensive makeup gas to be used.

A gas purification unit is also employed to maintain the gas. Obviously, if there is no in-leakage of moisture and the makeup gas is <1 ppm, there is no expectation of a fouled environment. However,

practical glove boxes are subjected to practical realities such as equipment transfers into the box and, less desirable, leaks. Off-gassing of water and oxygen is not usually expected except for very exceptional chemistry (e.g. electrolytic reduction of oxide species which might involve the production of oxygen gas) but in most cases should only create solid oxide species (such as the insoluble Li_2O or Na_2O or Ce_2O_3 in molten chloride salts) during these reactions. The gas purification system is well-known but deserves some discussion here since its operation, as the author has found, is rarely understood to most operators. Figure 2 is a schematic of the operational purification system in use.

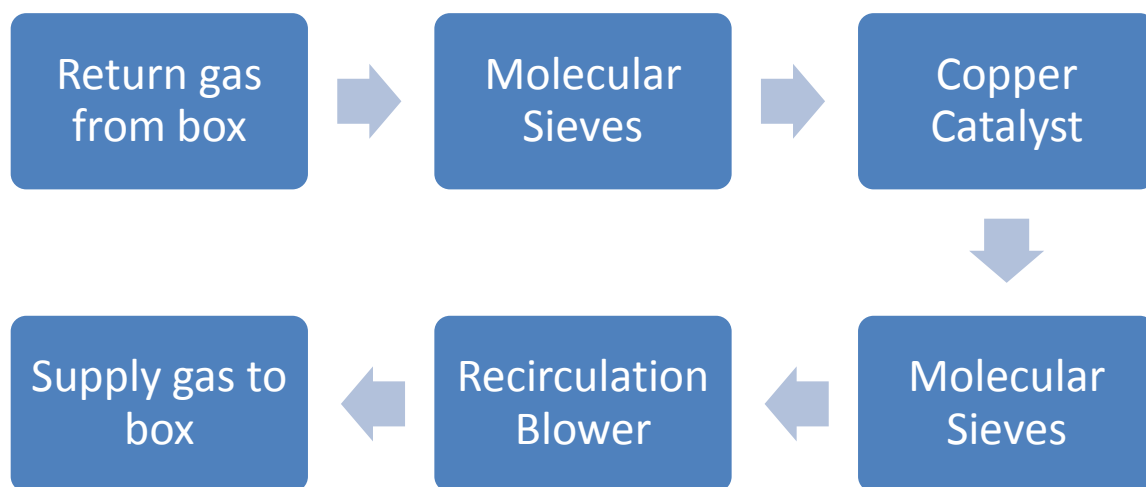


Figure 2: Purification Scheme for argon gas cleaning.

The box atmosphere is drawn into the purification column through a downcomer pipe and then dispersed upward via a bottom plenum to act as a gross particulate filter and allow for good mixing of the gas throughout the bottom of the volume of the column. The gas proceeds up through the 13X molecular sieves layer first to remove most water in the bottom third of the column. Then in

the middle third layer of copper catalyst, this finely-dispersed copper on an inert material (e.g. alumina) is used to scavenge the oxygen. For this system, it is the BASF R3-11G. While copper oxidizes somewhat quickly, without sufficiently high surface area metallic or 'lumped' copper would become exhausted and be of little practical use in a glovebox. Therefore, this high-surface area copper allows for fast reaction of oxygen over a longer operating lifetime (which is a typical 9 to 12 month cycle for most applications). Then the gas proceeds upward into the upper third layer of molecular sieves which strips out the remaining water. Typical dewpoints of less than $-100\text{ }^{\circ}\text{C}$ can be achieved with properly-prepared molecular sieves. This results in a glovebox with an operating atmosphere of $<1\text{ ppm}$ water and moisture (and, in reality the MU Chemical Engineering department glovebox can achieve operating dewpoints of less than $-120\text{ }^{\circ}\text{C}$ and $<100\text{ ppb}$ oxygen easily).

A regeneration of the column is necessary from time to time as the molecular sieves and copper catalyst become exhausted. This is achieved by using either hydrogen gas or carbon monoxide, although hydrogen is usually preferable to CO due to its acute toxicity. A mixture of 5% H_2 in Ar is used to reduce the catalyst by preferentially scavenging the oxygen. Although this reaction is thermodynamically favorable at room temperature, it proceeds faster at higher temperatures so an electric heater is used to ramp up temperature in the column first before the hydrogen gas mixture is used. Technically, the column heats up over three hours and comes to about $160\text{ }^{\circ}\text{C}$. Then, with the heater still on, the 5% hydrogen in argon flows through the column at about 15 L/ min at 6 psig which should not appreciably cool the column but still act to purge the oxygen from the reduced copper and, at these elevated temperatures, blow hot gas over the molecular sieves to purge the water. The oxygen scavenging by hydrogen is exothermic and that heat is then added to the column promoting drying of the sieves. Once this is accomplished, a vacuum of approximately 10^{-2} Torr is applied to the column to remove all volatiles and water residue on the hot column but no further

power is applied to the heating coils. Then, in the final cooling stage, box gas is used to backfill the column and the heat in the column decays to roughly atmosphere in about 4 hours. The entire cycle is 13 hours in length and should generate approximately 150 mL of liquid water at the exhaust vent, if collection is required, signifying a successful removal of liquid water and oxygen from the sieves and the copper, respectively.

With a glovebox whose atmosphere must be kept pure, it is obvious that a sampling system is necessary. A NYAD, Inc. moisture and trace oxygen analysis system is employed using a Thomas compressor-vacuum pump to drive flow through the system. This pump uses a diaphragm chamber to control flow and prevent contact with the outside air with a gasket seal which is crushed by four bolts at 40 ft-lbs of torque. For leak checking, this system is difficult since it cannot be easily isolated from the main chamber. However, with sufficient back pressure applied via a calibration port at the rear of the Glovebox Control Panel, one can apply some pressure and test the diaphragm and sealing system. The diaphragm itself has an operating lifetime of about 3000 to 6000 hours, depending on usage. In the present application, it runs continuously and should be leak checked or replaced 3 or 4 times a year to meet this requirement.

3.2 Chemical Reactor Equipment

3.2.1 Electrochemical Reactor Vessel

To perform the electrochemistry, a furnace to heat the samples was supplied from Omega Engineering which is a 220 VAC, single-phase, 900 Watt vacuum-formed ceramic fiber using helically-wound nichrome wire. The furnace controller is a digital PID compact system that can ramp temperature to 450 °C \pm 1 °C in under an hour with excellent stability during all operations. Additional temperature control is achieved using Kaowool[®] ceramic wool as a reflective heat blanket at the top and bottom of the furnace. Control is maintained by feedback through a K-type thermocouple inserted into the space between the reactor crucible and the furnace and electrically-

insulated using a quartz tube since contact with the outer sheath of the thermocouple can short out the windings of the furnace, which was sufficient to destroy a furnace before: even with safety fuses utilized.

The chemical reactor itself is a concentric set of CoorsTek® high-alumina crucibles (Sigma-Aldrich). A larger crucible encloses a smaller crucible in which the salt systems are loaded. This larger crucible performs three functions: 1) it provides a stable support of the salt-bearing crucible, 2) it provides a thermal mass that tends to mitigate temperature fluctuations and 3) it provides a stable location to position the thermocouple sheath properly and prevent excessive movement during operations.

3.2.2 Counter and Working Electrodes

The counter electrode (CE) is a 99.999% pure Pt wire (0.020" dia) from California Fine Wire wound to a spiral at the end that dips into the melt at an inner diameter of approximately 0.125". The upper portion of the wire is a porous alumina tube, typically employed for thermocouples, to give the wire some rigidity. The working electrode (WE) is a 0.8 mm diameter tungsten wire from Small Parts.com. The tungsten wire is cemented into a high-purity, non-porous alumina tubing with Zircar® alumina cement and cured at 650 °C for at least an hour. This configuration allows for a tight seal around the tungsten to maintain a constant surface area during operation. Additionally, after each electrochemical operation, the electrode is removed from service, the salt cleaned using de-ionized water (18.0 MΩ, nominal) and then resurfaced using 320 grit SiC paper on the polishing wheel to prepare for the next operation.

3.2.3 Reference Electrode

The reference electrode (RE) is perhaps one of the most important aspects of modern electrochemistry since it helps to maintain a precise WE potential. A RE is an electrochemical cell whose potential does not change as a function of current flow because its activity does not change. This means that a good electrode needs to be electrical contact with the electrochemical cell system

but should not permit the concentration to change appreciably. For aqueous systems, silver-silver chloride (Ag/ AgCl) reference electrodes maintain contact with the electrochemical system with either a small capillary opening or a porous glass, such as Corning® Vycor. Commercially-available electrochemical systems will generally employ this porous glass since these can be easily replaced when fouled by contaminants.

In molten salt systems, thin-walled quartz, glass or Vycor is used as the membrane. The use of glass is desirable since it can be easily obtained and then blown to a thin (<0.5 mm) thickness appropriate for electrical contact with the salt. This was performed by Bockris and co-workers with good results.³⁸ However, this is used as a disposable electrode since the membrane will no longer have the fracture toughness to endure more than one freezing cycle of the salt.

Vycor is therefore an obvious choice. This material actually comes in two standards, or “Codes”, according to Corning. The Vycor that is the porous type for electrochemical use is the Code 7930. The other is Code 7913. It is not nearly as porous and was found to not exhibit any desirable electrical characteristics for electrochemical work. That is, it does not seem to maintain electrical contact with the cell. Further difficulty was encountered when it was discovered that Corning has discontinued manufacturing of the 7930 and there are no manufacturers that make it (or equivalents) into tubes—just frits and plugs.³⁹

As a result, attention was turned to work that had been published⁴⁰ from Idaho National Laboratory on a simplified reference electrode for molten halide system use. They previously had been using Vycor as a membrane but in a much more complicated fashion; as it became apparent in their experience, Vycor itself becomes ‘electronically conductive’. This means that if the RE conductor touches the walls of the inside of the membrane, the electrode shorts. An insulating (alumina) sheath was needed to hold the electrode in place and into the electrolyte within. Recall that Vycor is

still a glass: it is still very brittle even at temperature so it is never unreasonable to assume that a new one will be needed. All of this work meant that if the RE needed to be replaced, it would have to be manufactured by a technician working in a glovebox. This complicated design is then further complicated by the loss of dexterity and fine motor control working in a glovebox. The INL researchers also remarked that the loss of experience in assembling reference electrodes was affecting quality and a new design was needed.

The new, simplified design required a completely 'new' material: mullite. Mullite, named for an island in Scotland on which it was first discovered, is $3\text{SiO}_2\text{-}2\text{Al}_2\text{O}_3$: a ceramic and glass (quartz) mixture. This material is manufactured as a corrosion-resistant and thermally-stable sheath for thermocouples used in extremely unforgiving environments. Mullite for these purposes is manufactured by Arklay S. Richards, Co., in Newton Heights, MA.⁴¹

The first time and place of the employment of mullite in an electrochemical system are not known however it is used^{42, 43} as early as 1961 as a reference electrode material. Mullite in chemical research has usually been limited to high-temperature reaction crucibles due to its stability but there are some papers using mullite as a membrane, though not in a formal reference electrode.

Mullite exhibits excellent characteristics for reference electrode membranes: it is non-porous but maintains electrical contact with the melt. Although it is electrical contact, it does not conduct electricity. Mechanically, mullite is preferable to glass or quartz since the likelihood of shattering on an accidental drop in a glovebox is low. However, what was found to be a problem was thermal stresses placed on the material. If the mullite tubing which contains its own electrolyte is cooled or heated rapidly, brittle failure of the membrane can occur. To avoid this, procedural changes to allow a soaking time during heatup and during cooldown. This seems to have avoided subsequent failures.

Compared to the complex design required for a quartz or Vycor tube membrane RE, a mullite membrane is a major improvement. The use of mullite provides a simplified design and a rapid construction of a reliable and useful RE. Figure 3 is a representation of the RE used here based entirely off of the design from the INL group.

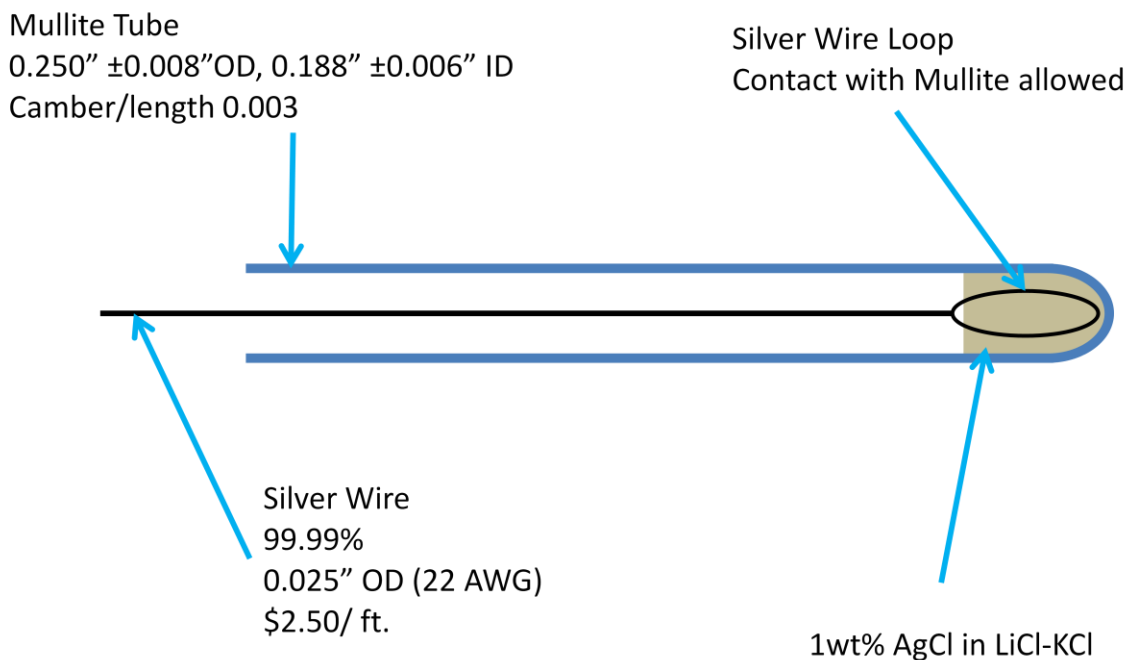


Figure 3: Simplified Reference Electrode in use at MU Chemical Engineering.

The mullite tubing comes with a rounded edge as standard issue, but other terminations are available. A 1-wt% AgCl (Sigma Aldrich, 99.998%, anhydrous beads) in the eutectic mixture of LiCl-KCl (44-wt%LiCl in KCl, anhydrous beads) is prepared in the glovebox by melting at 450 °C and then frozen. The solid mixture is then crushed and powdered in a mortar and pestle to a fine powder that can be poured into the mullite tubing. This powder is then melted within the tubing at 450 °C and a silver wire is dipped into the liquid salt solution. Silver wire (California Fine Wire, Grover Beach, CA), 99.99% is used as the electrical contact as well as the reference state of the silver. This process is not only simple in concept but easily executed within a glovebox where control is limited.

3.2.4 Electrochemical Cell System

With all of the electrodes assembled individually, the electrochemical cell itself is constructed by holding the electrodes in an inert, non-porous, temperature-resistant material that can be easily machined. The choice in this application was macor (McMaster-Carr) which is considered a glassy-mica. Figure 4 is a schematic of the electrode system assembly.

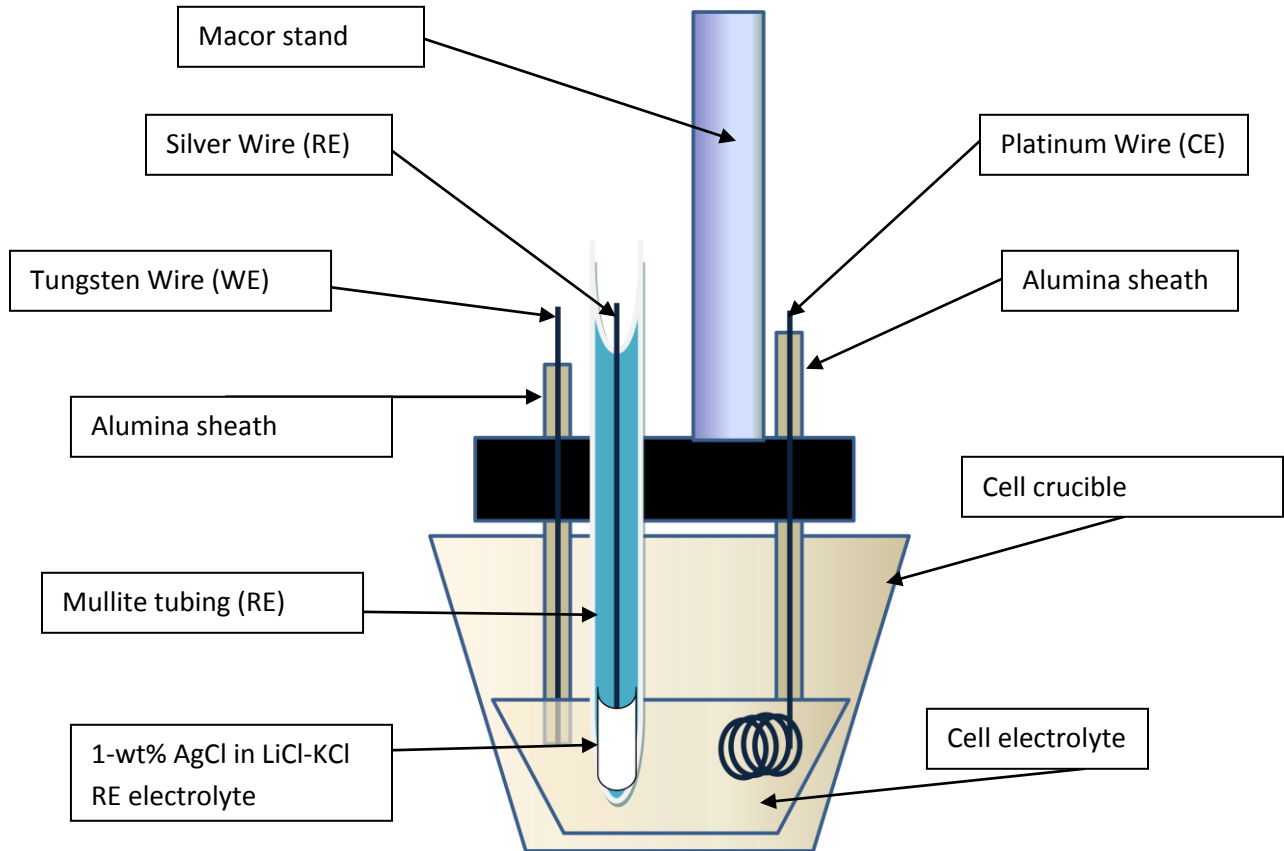


Figure 4: Electrochemical Cell Electrode Assembly

The WE and CE are held in place by alumina sheaths that maintain rigidity and distance. The RE is held in place by the use of a binder clip with eventually needs to be replaced due to the heat slowly reducing the spring-force. Configurationally, this design maintains the distance minimized between the RE and WE, and thus get the best indication of the potential on the WE and distance maximized between the WE and CE. The aluminum cement is used in some places to hold the electrodes in

place but this should be minimal since it eventually breaks down in the presence of the chloride salts (and in HCl solutions, if used as a cleaning agent) and has to be reapplied.

3.3 Sample Preparation

For each sample loaded into the electrochemical cell, the alumina crucibles are cleaned thoroughly with hot (60 °C) aqua regia (prepared from Fisher Scientific, 75% HNO₃, 25% HCl) for several hours. This is sufficient to dissolve any organics as well as all trace metals from the containers. The crucibles are rinsed with deionized water (18.0 to 18.2 MΩ-cm purity) and placed into the glassware oven to bake out all residual moisture for at least 3 hours. Still hot, the crucible is introduced to the glovebox to prevent moisture from being collected into the pores of the crucible during transfer.

All electrolyte was purchased from Sigma-Aldrich (44-wt% LiCl in KCl, 99.99% trace metals basis, anhydrous beads) as sealed glass ampoules to maintain a moisture-free transfer. This was used without further purification. The choice for this material is simple: there is a lot of operating experience with this mixture and it precludes working at 650 °C such as with straight LiCl.

Cerium chloride (Ce(III)) was purchased from Sigma Aldrich (99.99%, trace metals basis, anhydrous beads) and used without further purification. Again, this salt was also delivered in glass ampoules to prevent moisture infiltration until ready for use within the glovebox.

3.4 Analytical Methods

All electrochemical analyses were performed using the electrochemical cell (described above) connected to a Gamry 300G Potentiostat used as a PCI card on a Windows XP machine. It is a completely software-driven, self-contained system with a current limitation of 300 mA (well below the grand majority of experiments encountered here). The software package included allows for many different types of electrochemical experimental scenarios and is robust and flexible for all work here. To interface within the glovebox, since direct connections cannot be made, leads from

the Gamry were connected via banana jack plugs to a sealed bulkhead penetration bundle junction box external to the glovebox. Although this increases the propensity of EMI (electromagnetic interference) pickup during operation, it was necessary for proper connection. Gamry proposed a method to reduce noise (on the WE current measurement) by shunting AC signals (measured to be 60 Hz, which was expected) on the RE to the CE. To do so, a 10 μ F electrolytic capacitor (though without regard to polarity) was connected between the CE and RE leads at the junction box. This did improve the noise in the current signal but did not completely solve the problem. Examining the noise issue further, the fact that most of the current-carrying conductors of the entire system were enclosed in the stainless-steel glovebox meant that stray EMI from external system was probably negligible (since it acts as a giant Faraday cage). Through troubleshooting, it was determined that the noise was generated as a result of the furnace as it could be visible when the controller had a error signal to demand power applied to the furnace. While the furnace could be de-energized during measurements, this is a clumsy and awkward way to operate and, more seriously, a constant temperature assumption will not be accurate. When the Gamry system/ PC were powered, however, from the same electrical distribution system as the glovebox, the noise was no longer an issue and the capacitor was made redundant. In summary, noise from molten salt (i.e. high temperature) electrochemical systems is a very big issue since the very device keeping the system molten can be generating noise that is detrimental to clean data collection which can affect the limit of detection.

Following electrochemical work, other data were gathered to get a better idea of what was going on. For example, Ce metal that was deposited onto tungsten foil was imaged using Atomic Force Microscopy (AFM) and other metals were examined and imaged using Auger Electron Spectroscopy (AES) which are two tools available in the PinheroLAB.

Chapter 4 Results and Discussion

4.1 Reference Electrode performance and characterization

The use of the reference electrode is only as good as it is repeatable as well as usable. Here, several runs using the Mullite Membrane Silver-Silver Chloride (MMSSC) RE were performed with known concentrations of cerium ions in a molten salt solution.

Before using the new mullite reference electrode, greater understanding of how it would respond in a chloride melt was required since literature involving its use is very limited. Only the work at INL was known to the author at the time of this writing. However, based on the performance in this application, the MMSSC RE is suitable for further use.

Samples, designated A, B and C as well as a 'blank', were approximately 20 g of salt (44-wt% LiCl in KCl eutectic) with approximately 50 ppm Ce in each, except for the blank. Table 4 gives the quantitative information for each of the samples.

Table 4. Concentration Data and uncertainty for each sample.

Sample ID	Concentration of Ce added (ppm)	Uncertainty in Concentration of Ce added (ppm)
A	34.11	5.00
B	56.77	4.99
C	40.07	5.01

Figure 5 (a through d) are the cyclic voltammograms (CV) taken at various scan rates of each sample with the MMSSC RE. The scan rates are shown with different colors: red for 10 mV/ s, gold for 25 mV/ s, green for 50 mV/ s and blue for 100 mV/ s (the higher the scan rate, the 'bluer' the coloring).

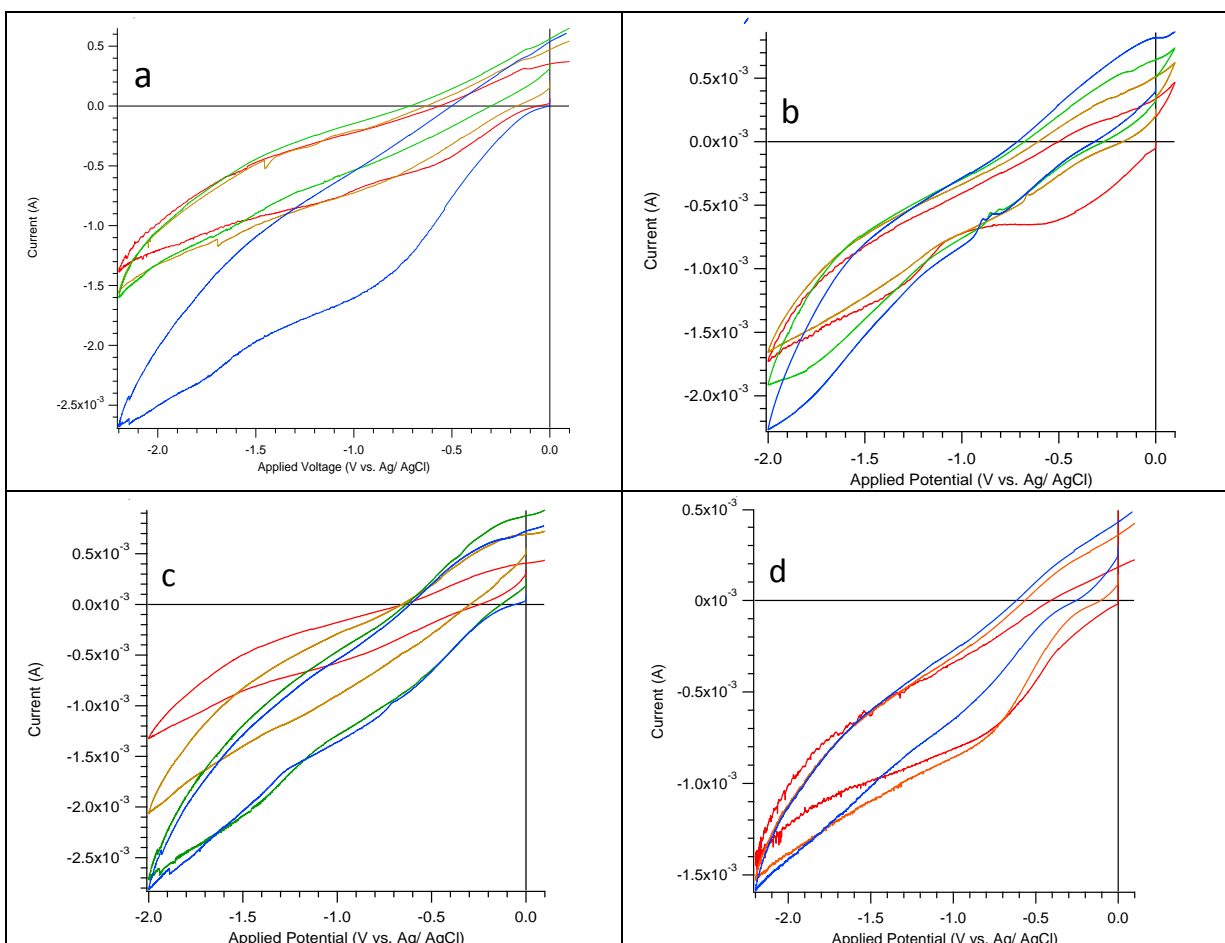


Figure 5. (a) Sample A, (b) Sample B, (c) Sample C and (d) is a blank (containing no Ce added).

While the plots themselves look fairly similar, the proper trend of an increasing magnitude of current is observed. This is because faster scan rate avoid charging effects in the salt and higher currents are attainable before a double layer capacitance is established.

Quantitatively, we can now examine the current magnitude at (almost) any arbitrary working electrode potential. Theoretically, any value might be useful however in real electrochemical systems there could be many sources of interference that affect the quality of the current, not to mention external interferences, such as EMI. It is best to select a potential that is near E^0 (the standard reduction potential with respect to the reference) and not more cathodic than that. This is

due to the fact that, if in any other case than a truly reversible reaction, reproducible results would not be possible. Table 5 gives the data associated with each sample for the scan rates shown. Uncertainty in the current magnitude is estimated at 1 μA as this is maximum deviation observed in the CV.

Table 5. Current magnitudes for each sample as a function of scan rate.

	Sample A 34 ppm \pm 5 ppm	Sample B 56 ppm \pm 5 ppm	Sample C 40 ppm \pm 5 ppm
Measured at -2.0 V vs. Ag/ AgCl	Peak Current (mA)	Peak Current (mA)	Peak Current (mA)
10 mV/ S	1.376	1.729	1.323
25 mV/ s	1.573	1.660	2.056
50 mV/ s	1.595	1.913	2.715
100 mV/ s	2.679	2.266	2.808

The correlation of these data is close; that is, for the most part, increasing current is seen with increasing scan rate as well as increasing bulk concentration. For a truly reversible reaction, these systems would demonstrate Cottrell behavior. The Cottrell equation states that the magnitude in current observed in a chemical system, with no other changes in the bulk concentration, should increase with the square root of the scan rate (in s^{-1}). Figure 6 shows these data along with trend lines and their associated equations.

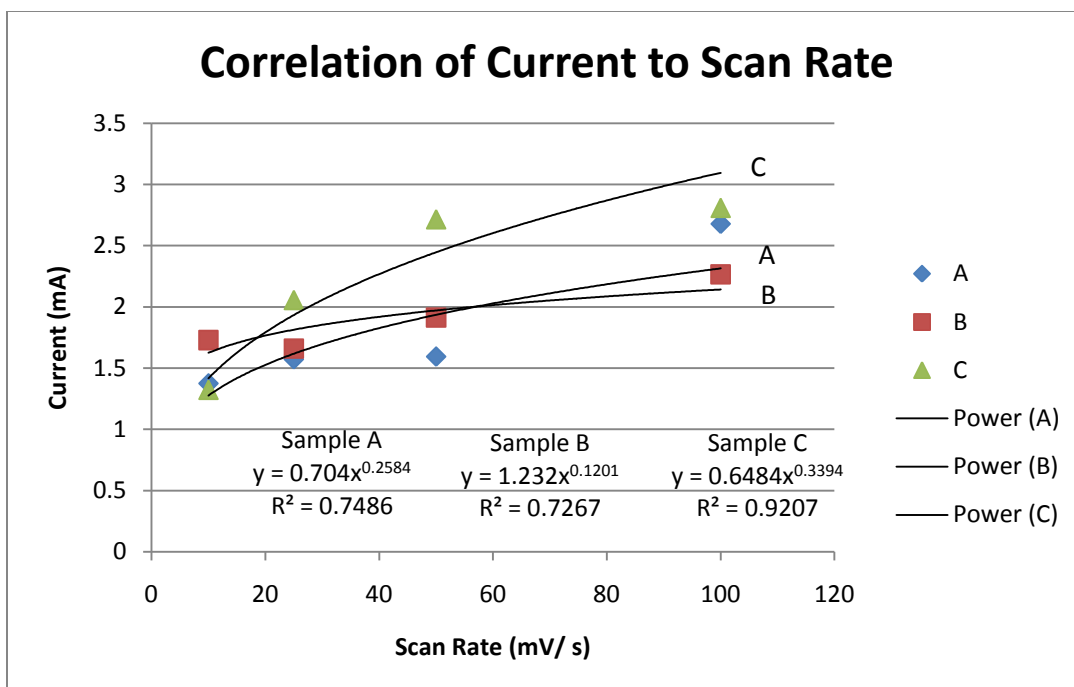


Figure 6. Plot of current magnitude as a function of the scan rate.

Each sample exhibited ‘gentler’ characteristics than that of truly Cottrell square-root behavior. This is most likely the case since the Ce(III) to (0) is not truly reversible and therefore will be slower than the equation, since the other variables are held constant. Each sample was run at the same temperature so no deviation in the diffusion coefficient should be seen.

However, between Sample A and B, a new RE had to be constructed as the previous one shattered on the last run and had to be removed from service. Since all these data (this includes the CV) between the samples correlate well, it can also be seen that the RE seem to agree with each other.

The question then remains, how well do these reference electrodes correlate? To answer this, some other standard might be used. Good data can be obtained from using a simple Pt wire immersed in the melt. Platinum in molten chloride systems is quite stable and is considered a good quasi-reference electrode (QRE). QREs are RE that exhibit some characteristics of a reference but will not nearly be as robust for the long-term. Platinum, though somewhat noble in these molten chlorides,

does eventually corrode. A little corrosion is actually desirable in this case since we require that the concentration of Pt(II) remain as constant as possible to maintain the potential on the Pt wire as possible with respect to the WE. Since the corrosion rate is quite small, this small amount of Pt(II) that exists in the melt is, for short exposures, stable. However, long-term soaking should be avoided or sample contamination will occur.

The same samples were then analyzed using the MMSSC RE and the Pt QRE (but in all cases, the Pt was used second to avoid spurious signals from Pt in the CV). To give a quantitative answer as to how well these correlate, the standard deviation in the currents between each sample (at a given scan rate) are computed and then plotted as a function of potential. Figure 7 demonstrates the magnitude of deviation between samples as a function of applied potential for each scan rate.

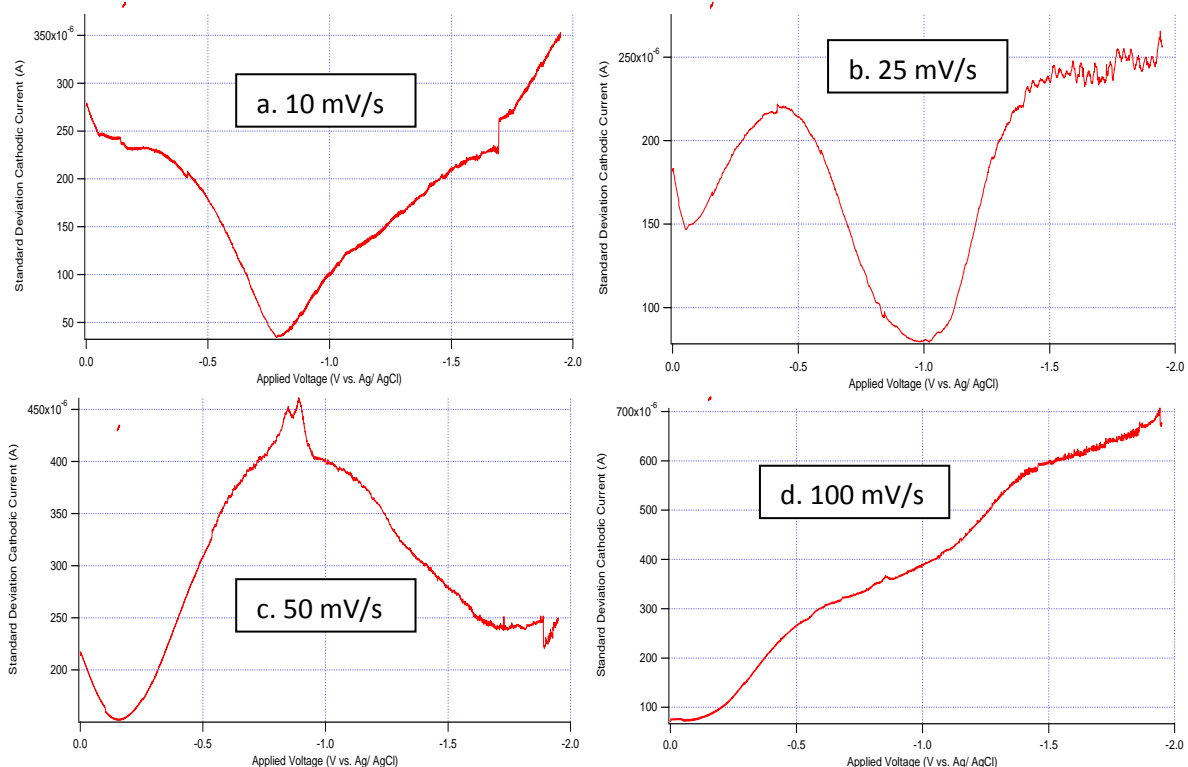


Figure 7. Standard deviation in the current signal (between Samples A, B and C) as a function of applied potential using the MMSSC RE.

Perhaps the most interesting aspect of these plots is the large fluctuations over the cathodic region of the CV. However, careful examination shows a standard deviation of a few hundred μA at maximum. For the region of interest at the reduction of Ce(III) to Ce(0), the standard deviation varies too widely: usually around $300\ \mu\text{A}$ but for $100\ \text{mV/s}$, as high as $700\ \mu\text{A}$.

For the Pt QRE, the results of the standard deviation calculations are shown in Figure 8.

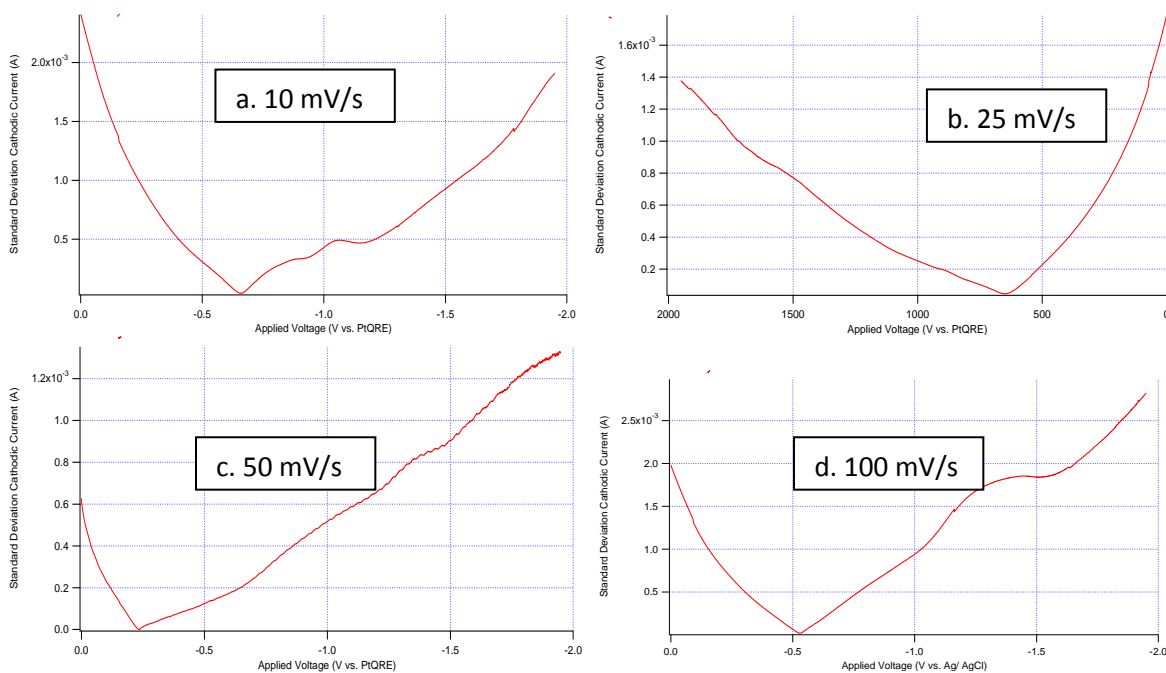


Figure 8. Standard deviation in the current signal (between Samples A, B and C) as a function of applied potential using the Pt QRE.

The contrast in the curve shape (to the mullite RE) is startling. These plots exhibit sharper behavior moving from 0 to -2.0 V (vs. Pt(II)/ Pt(0)). Compare the magnitude of these deviations to that of the Ag/ AgCl RE and there is about an order of magnitude improvement in the deviation when using the MMSSC RE.

Based on these data obtained on these samples, as well as the background information regarding the material stability, it is reasonable to say that the mullite membrane reference electrode for the Ag/ AgCl is an acceptable choice for a reference electrode. Practically, since molten chloride

research is almost always reporting data with respect to the silver-silver chloride couple, this makes things easier since a conversion is not needed.

Whereas quartz (and, therefore, Vycor) does exhibit some electrical conductivity in a molten chloride system, mullite does not. This is true because the silver wire can be in physical contact with the mullite tube during operation (and it is because the preparation procedure requires it to be bottomed in the manufacture). The outside of the mullite is virtually non-porous: water tends to bead-up as well as the evidence that the manufacturer considers porosity to be detrimental to mullite's use in corrosive media. Why, then is mullite a good candidate material in the first place for reference electrodes? The literature is not clear on how anyone determined that mullite was considered.

To answer this question, some basic aspects of reference electrodes need to be reviewed. A membrane for a reference electrode needs to maintain the activity (concentration) of the species within it to maintain the same potential on the electrode with respect to the WE. At the same time it needs to remain in electrical contact with the rest of the cell. This means that the electric field must be able to be supported through the material, not so much charge (although that is how capillary-based reference electrode membranes function).

Material analogous to this description is a dielectric. Dielectrics are, by definition, materials that allow for bound charges to move only within that medium as a response to an applied potential and become polarized. If the mullite membrane material can become polarized, it would exhibit behavior that is consistent with supporting an electric field with little conduction.

Direct testing of the reference electrode material is not easily accomplished. Electrochemical Impedance Spectroscopy (EIS) is a method by which one can obtain impedance and phase information from a system and then drawing some conclusions based on a 'reasonable' physical

description of the system and hopefully, one can model it with resistive, capacitive and inductive elements. While this sounds somewhat straight-forward, there are literally infinite combinations of resistors, capacitors and inductors in an equally infinite number of configurations (series, parallel) to model phase and magnitude of impedance. This is because there are no direct ways of removing other sources of capacitive reactance and inductive reactance from an electrochemical cell. We can start by using some basic elements for some reasonable assumptions about electrochemical cells and this has been done in the past already.

While it should be noted that capacitive characteristics in electrochemical cells are 'easily' explained (i.e. double-layer/ Helmholtz layer), inductive effects are far more elusive. Inductive characteristics are, by definition, when current leads voltage (or potential) to give a positive phase angle (unlike capacitive effect which is the opposite). One can easily envision the capacitive nature but not so with the inductive. Typically, in circuit theory, this would mean that changes in current are opposed since there would be a magnetic field that is generated due to that change in current as a function of time since an inductor is a coil of wire such that a magnetic field can be maintained. Obviously, there are no 'coils' of wire in an electrochemical cell so easy analogs are not found.

EIS was performed on molten salt samples containing cerium so that data could be generated to help explain why this may be so. It is not clear from these data what might be drawn to help elucidate the concept or even pose some possible explanation. For the most part, the electrochemical cell exhibits a capacitive nature: it is only at frequencies above 17 kHz that phase angle is positive. Most electrochemical work is carried out well below this frequency (the fastest scans that are typically performed are only a few cycles per second).

To see if mullite has some physical explanation for a capacitive nature, and therefore contains dielectric material, two elemental analyses were performed on 'virgin' mullite and mullite exposed to salt (with Ce added).

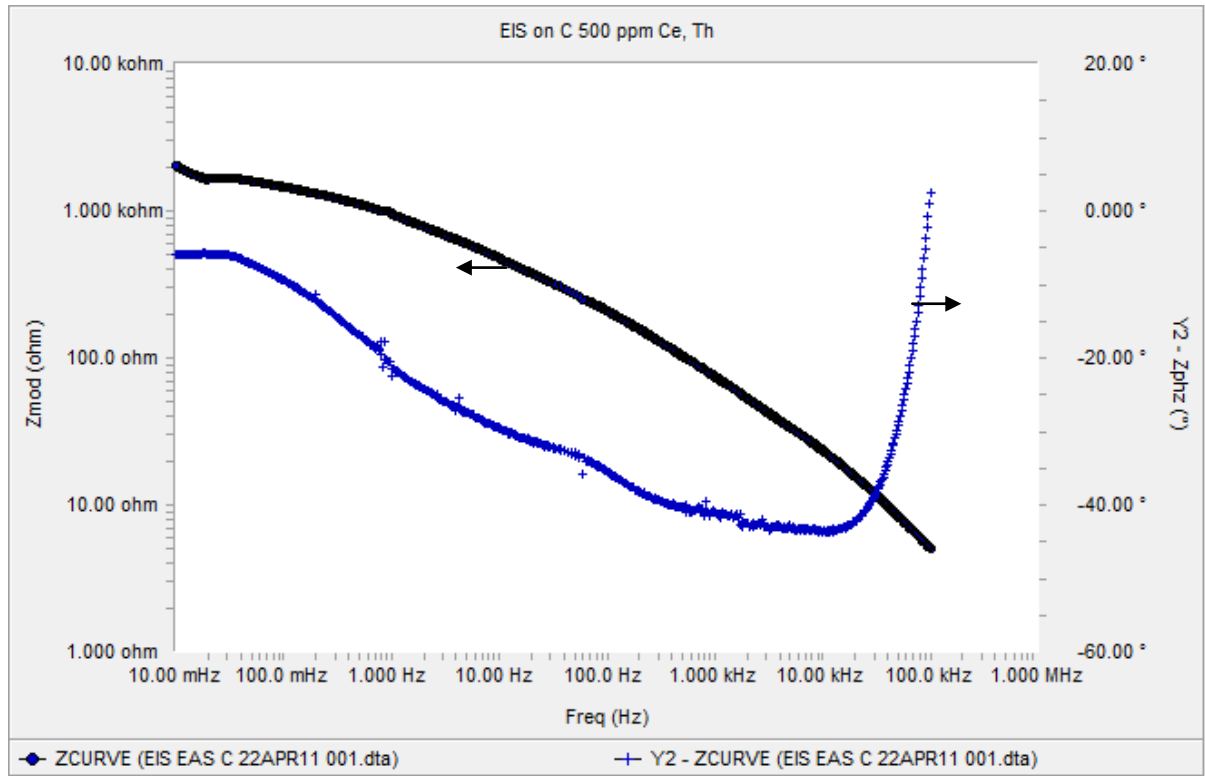


Figure 9. Bode plot of 500 ppm Ce with Th turnings added following anodic dissolution.

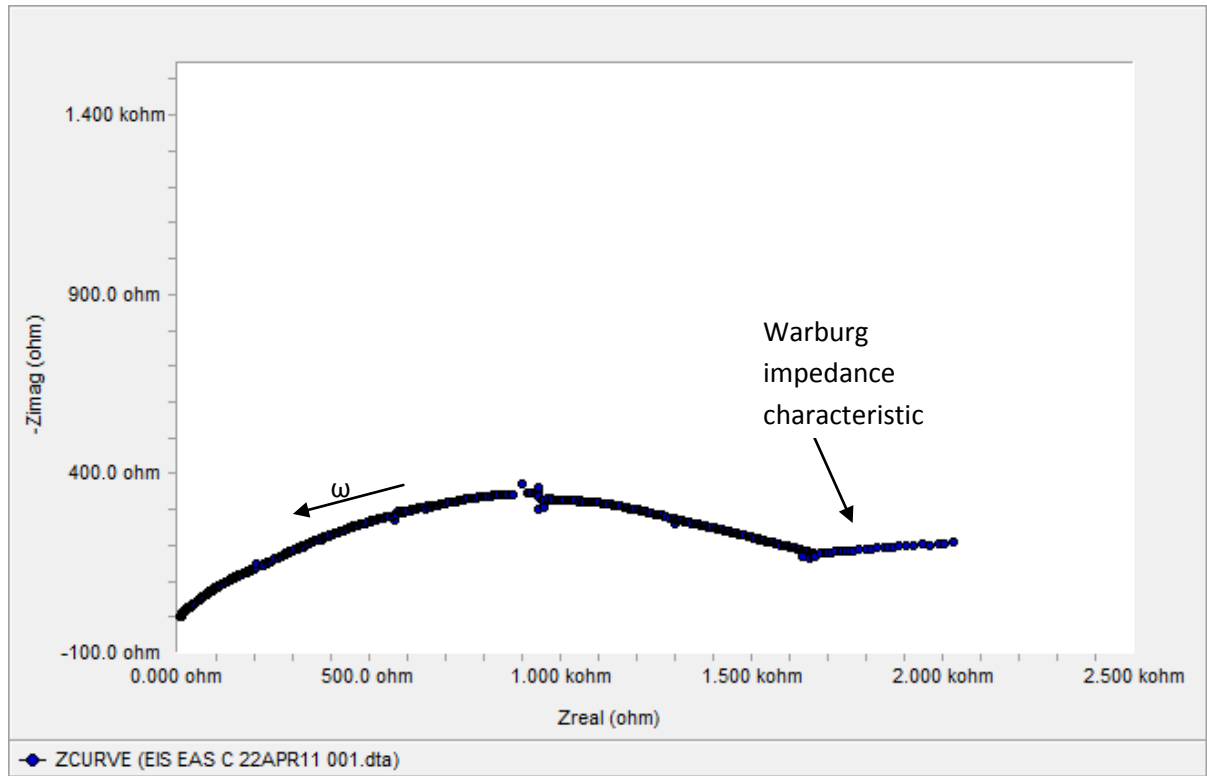


Figure 10. Nyquist plot of 500 ppm Ce with Th turnings added following anodic dissolution.

X-ray Fluorescence (XRF) is a non-destructive, mostly qualitative, elemental identification method. By using a beam of x-rays, inner-shell electrons are excited and then relax giving a characteristic photon emission that can be used to identify elements rapidly. It gives no information regarding chemical structure and it cannot be used for all elements. An additional complication was the sample preparation. Samples need to be flat for XRF and mullite samples here are all round. This required the samples to be cut with a diamond saw. Figure 11 gives the results of the XRF analysis.

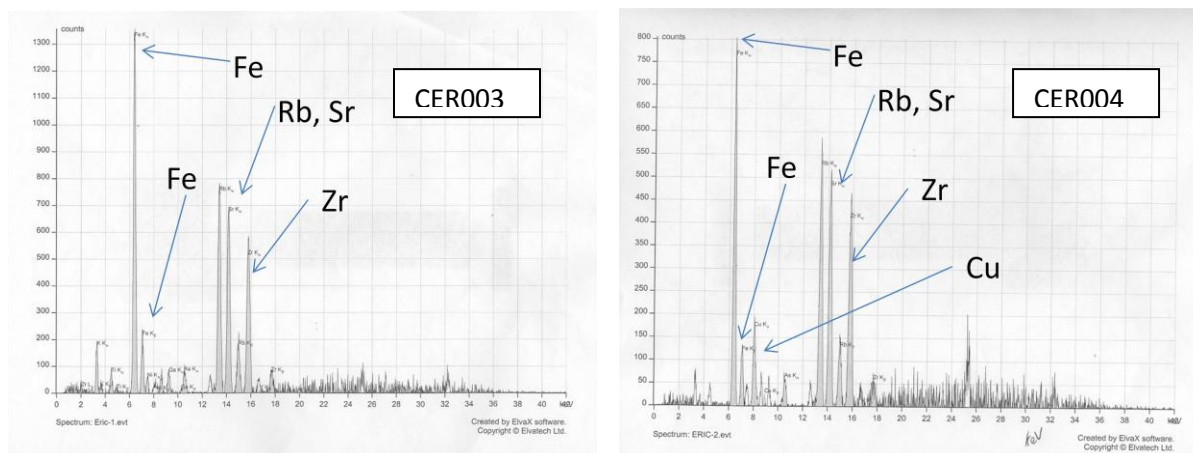


Figure 11. XRF results on sectioned mullite samples CER003, CER004.

From these results, the data give roughly the same result: a large contribution of Fe, Sr, Rb and Zr. The copper may be a false positive as this is most likely contamination from the diamond saw as it was used for sectioning copper samples in an unrelated research project.

While these data are somewhat useful, they indicate only relative intensities of fluorescence which could indicate relative concentrations. However, XRF has a major limitation in this application due to its ability to penetrate no deeper than 100 μm (as a general rule of thumb) but it is highly dependent on the density of the matrix.⁴⁴ XRF was a convenient test before samples were exposed in a neutron flux for Neutron Activation Analysis (NAA) to reduce any long-lived or high-energy radionuclides that could impact timely measurement.

NAA is a technique that utilizes a thermal neutron (<0.1 eV) flux to activate components, making radioactive nuclides whose decay chains and energies are discrete and well-known. These neutrons penetrate the samples completely and this technique is, for all intents and purposes, matrix-independent. Here at the University of Missouri, a 10-MW nuclear research reactor (the University of Missouri Research Reactor or MURR) provides a large inventory of thermal neutrons for a specific period of time. Then, the samples are brought to a high-purity Ge (HpGe) detector to resolve the

energies of the gamma photons that are emitted when these radioactive nuclei are decaying. The intensity of the lines, in addition to the energies and their abundances, can be calibrated using standards and then a quantitative result can be obtained. Figure 12 gives the result from NAA analysis on two separate samples (CER005, CER006).

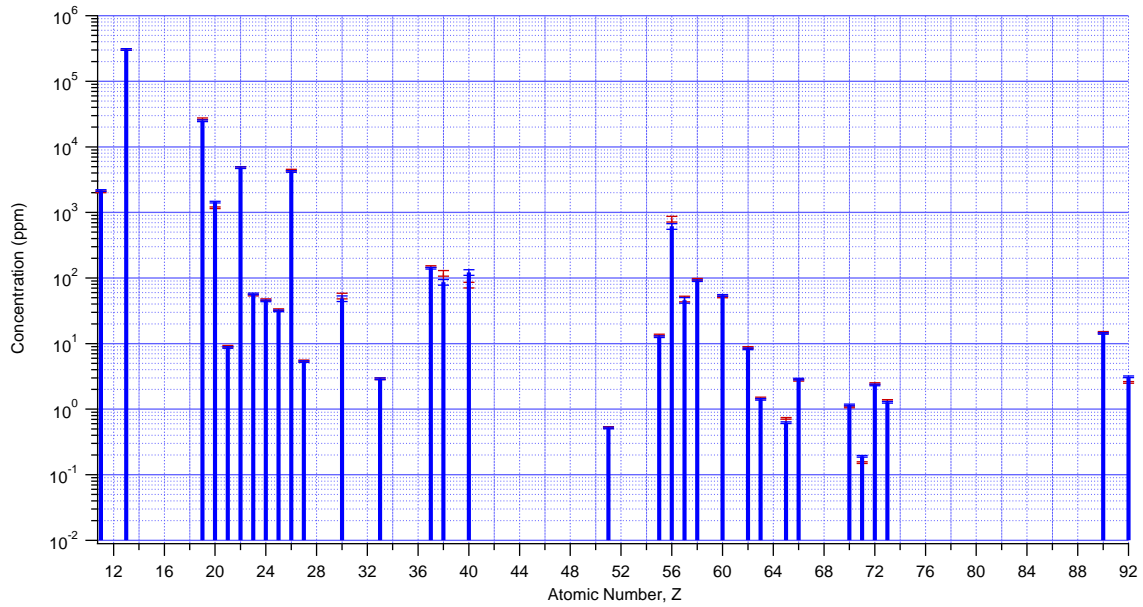


Figure 12. Concentration of various elements for samples CER005, CER006 (virgin mullite) from NAA.

Table 6. CER006 elemental composition and uncertainty in descending concentration.

Element	Z	Concentration (ppm)	Uncertainty (ppm)	Element	Z	Concentration (ppm)	Uncertainty (ppm)
Al	13	305102.8	9153.1	Mn	25	31.57	0.9
K	19	25072.5	752.2	Th	90	14.2974	0.4
Ti	22	4823.1	144.7	Cs	55	12.7546	0.4
Fe	26	4217.1	126.5	Sc	21	8.7590	0.3
Na	11	2154.3	64.6	Sm	62	8.3287	0.2
Ca	20	1432.5	43.0	Co	27	5.3136	0.2
Ba	56	615.4	61.54346	U	92	3.1132	0.1
Rb	37	141.09	4.2	As	33	2.9143	0.1
Zr	40	122.02	12.20196	Dy	66	2.8811	0.1
Ce	58	90.9127	2.7	Hf	72	2.3497	0.1
Sr	38	86.57	8.65731	Eu	63	1.4172	0.0
V	23	57.20	1.7	Ta	73	1.2722	0.0
Nd	60	54.1472	1.6	Yb	70	1.1578	0.0
Zn	30	48.62	4.86154	Tb	65	0.6232	0.0
La	57	45.8159	4.58159	Sb	51	0.5162	0.0
Cr	24	44.812	1.3	Lu	71	0.1912	0.0
				Ni	28	0.00	0

Figure 10 and Table 5 together show a good picture of what these mullite thermocouple tubes have as their impurities. From these data, it is clear that some impurities are not so trace at all and this can actually be the mechanism behind the usefulness of the these mullite tubes as electrode membranes. The uncertainty is determined from the analytical experience doing long-lived and short-lived NAA examinations.

Finally, if dielectric behavior is to exist, it may be of some value to assign a ‘weighting’ index to these elements based on their individual polarizabilities. As one goes down the periodic table in the alkali metals and alkaline earths (Group 1 and 2), we see an increasing trend in polarizabilities: the electron density is more easily deformed in the presence of an electric field with these atoms since these s-shells are far more diffuse for period 4 and 5, for example. By obtaining established values of atomic polarizabilities, one can see the biggest contributors below in Table 7.

Table 7. Concentration-weighted polarizabilities in mullite (Sample CER007).

Element	Polarizability ⁴⁵ (10 ⁻²⁴ cm ³)	Concentration-weighted Polarizability index	Element	Polarizability ⁴⁵ (10 ⁻²⁴ cm ³)	Concentration-weighted Polarizability index
Sc	17.8	147.3253	Ce	29.6	6024.879
Cr	11.6	469.9937	Nd	31.4	1201.044
Fe	8.4	33641.88	Sm	28.8	224.2483
Co	7.5	36.29025	Eu	27.7	36.81607
Zn	5.75	286.4018	Tb	25.5	14.9685
As	4.31	17.62187	Yb	20.9	19.80693
Rb	47.3	6277.036	Lu	21.9	3.21492
Sr	27.6	2317.15	Hf	16.2	36.03042
Zr	17.9	1111.644	Ta	13.1	15.97545
Sb	6.6	3.39174	Th	32.1	431.3598
Cs	59.42	726.4927	U	24.9	79.52064
La	31.1	1340.143			

From these data we can immediately see that Rb, Sr, Zr, Ce and especially Fe play a substantial role in the dielectric nature of the material. In the absence of other reasonable explanations, a capacitive nature of the mullite membrane seems appropriate.

4.2 Cerium Deposition onto Tungsten

Most of electrochemistry involves relatively small perturbations in the electrochemical cell. These perturbations are usually not intended to change significantly the chemistry. Beyond the analytical work is the practical work of extraction: the use of electrochemical methods to purify.

To do some deposition studies, the location of a reduction peak should be known within the chemical system. Using Cyclic Voltammetry (CV) and Differential Pulse Voltammetry (DPV), the reduction potential can be seen clearly. Figure 13 is the result of the DPV analysis. Note the sharp peak for the Ce(III) reduction to Ce(0).

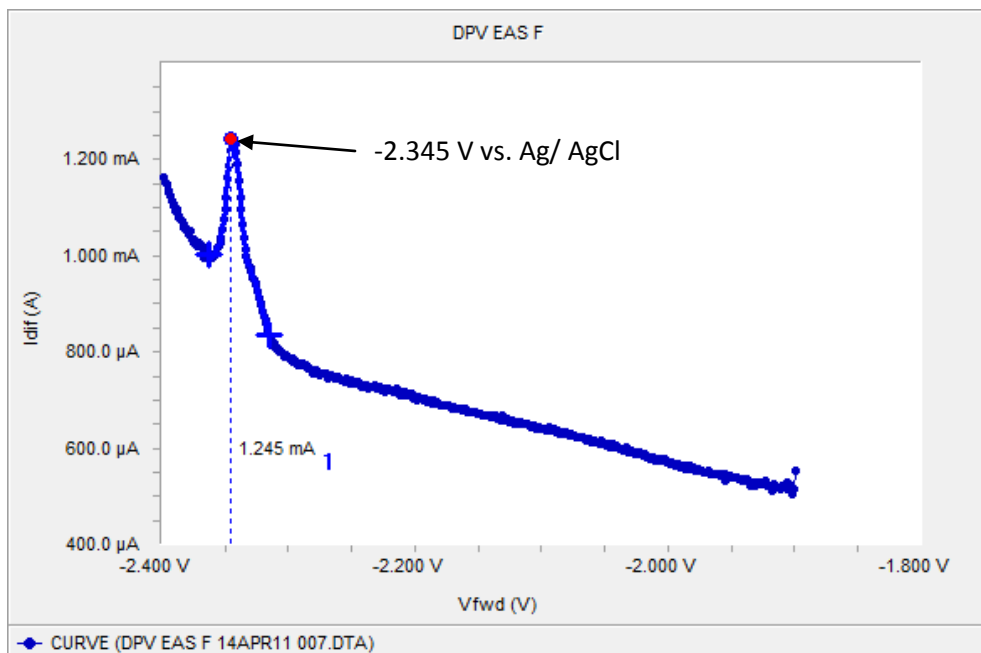


Figure 13. DPV on Sample F (Ce solution in LiCl-KCl) showing the Ce(III) to Ce(0) peak.

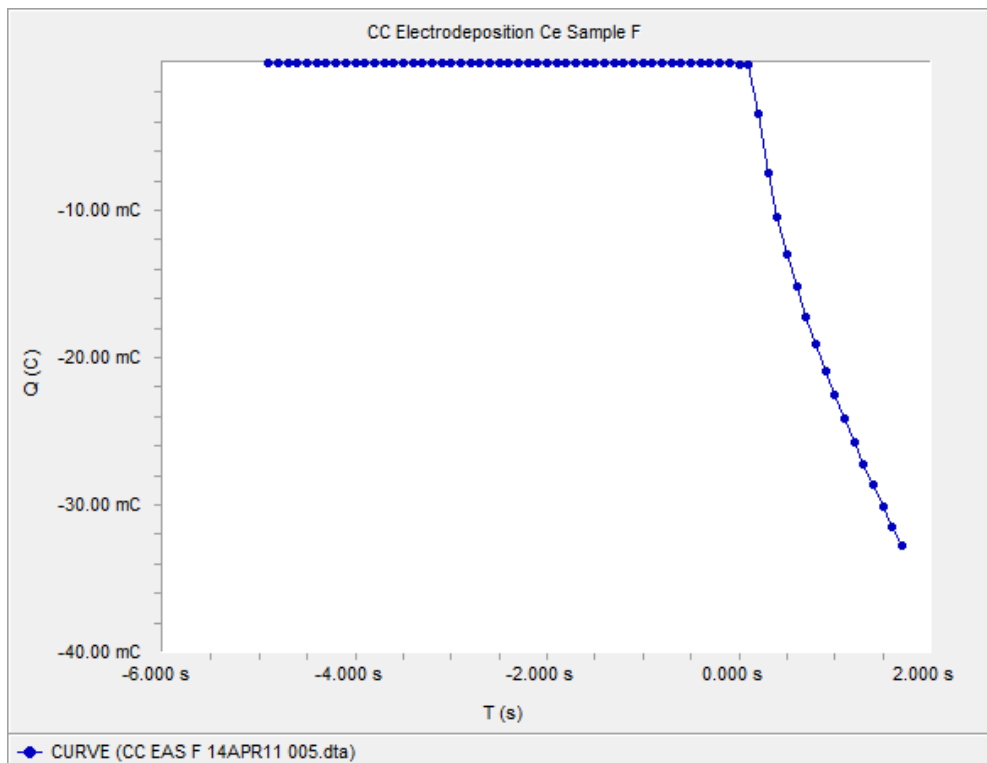


Figure 14. Chronocoulometry run for Sample F to extract Ce metal from melt.

For the deposition, Figure 14 shows the progress of the run. The system was programmed to stop at 30 mC for a constant potential at -2.300 V vs. Ag/AgCl. This value is slightly anodic to prevent

inadvertent deposition of Li or K metal as the salt's extent is only a few hundred millivolts more cathodic. While the electrochemical analysis was done with the standard working electrode, the deposition was performed using a tungsten foil. The surface area is approximately 1.0 cm^2 . Following deposition, Atomic Force Microscopy (AFM) was performed on the foil.

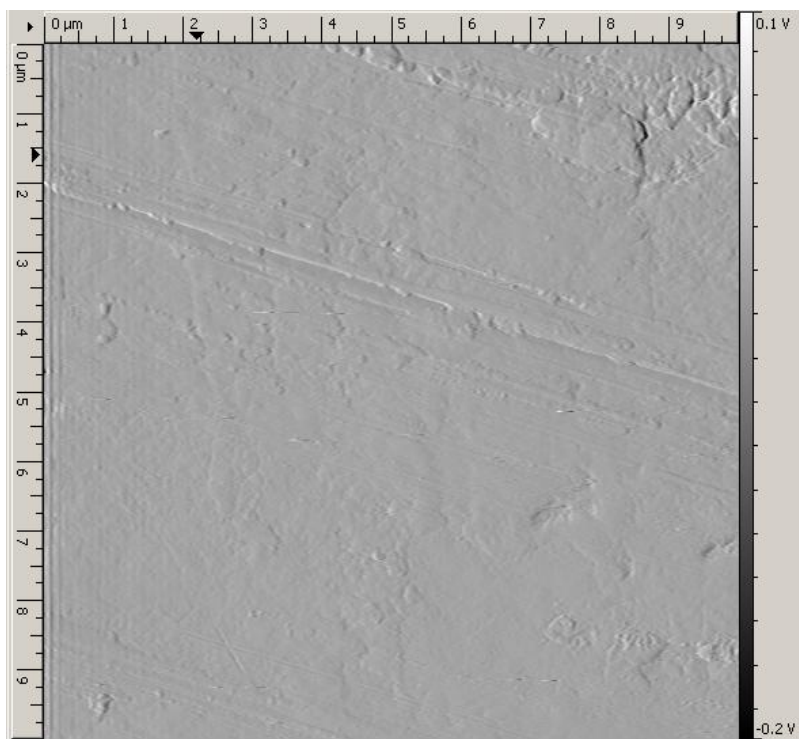


Figure 15. Tungsten foil blank.

Figure 15 is an AFM image(10 μm) of a representative tungsten foil blank to show the surface prior to molten salt immersion and electrodedeposition. Following deposition, the surface of the tungsten shows a remarkable change. This is given as Figure 16. There are interesting features, such as a 'bubbled' appearance.

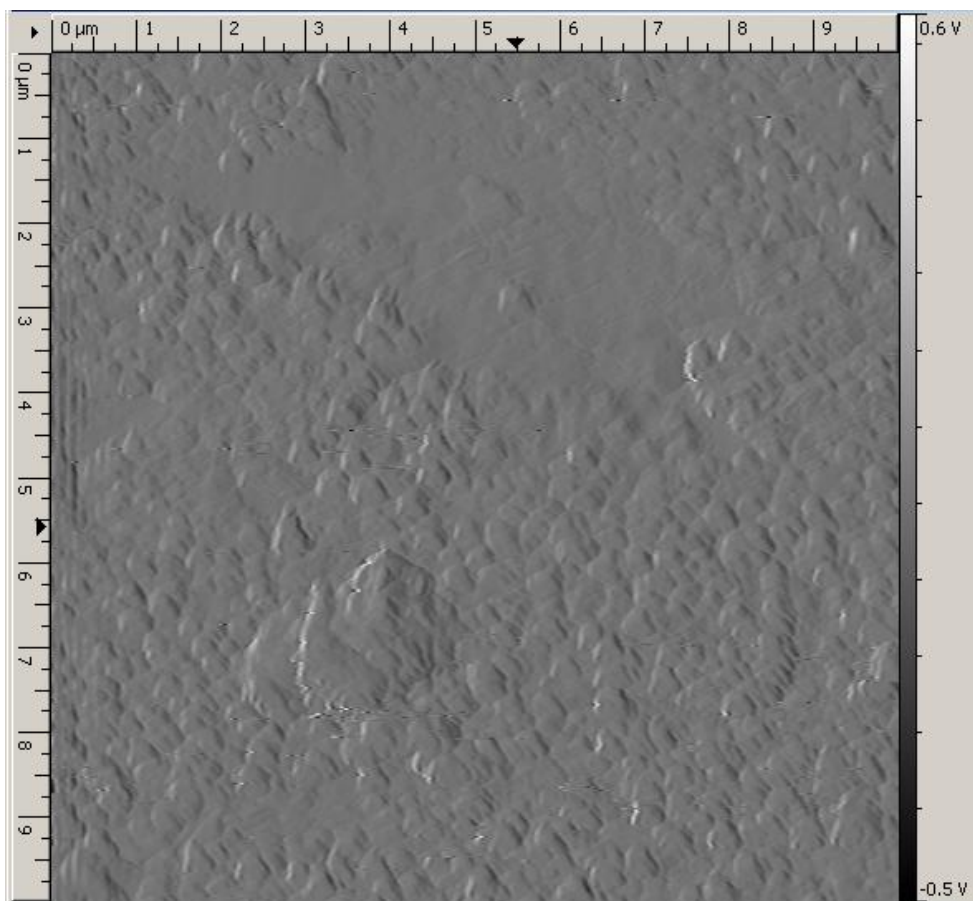


Figure 16. Tungsten foil after Ce deposition and salt immersion.

4.3 Electrochemical examination of Green Mill Tailings from Southeastern Missouri

An interesting technological use of molten salt electrochemistry is separation of specific species from a mixed collection. In southeast Missouri, the Pea Ridge Mine is an old hematite mine that may have some importance due to the lanthanide content. Rare Earths (RE), another name for the lanthanides, are the $4f$ electronic elements and are used primarily in high-strength magnets. These mill tailings are the leftover materials from the extraction of iron.

To have the material react in the melt, the green mill tailings must be in a chemical form that allows for dissolution in the molten chloride. To 4.9932 g of green mill tailings was added 150 mL of concentrated HCl and stirring at 80 °C. The material is then vacuum filtered using a Fisherbrand medium pore size P5 filter paper and collecting the filtrate in 95 mL of 19.1 M NaOH. Once the material was filtered (collecting the dissolved constituents and then neutralizing it) HCl was added to lower the pH to 3.58. This is necessary to ensure that there is a large chloride inventory for use in the molten chloride salt cell. This solution is boiled down into a peach-colored cake and dried in a oven at 130 °C. This material is then crushed in a mortar and pestle to a fine powder and labeled as GMT005.

The electrochemical cell is formed from 261.5 mg of GMT005 dissolved in 19.6489 g of 44-wt% LiCl in KCl at 450 °C. The sample was agitated to promote mixing and then the electrodes were loaded into the cell.

Chapter 5 Conclusions

The molten salt technology required for electroanalytical work as well as separations work has been improved. There is more work to be done in order to increase the sample throughput and use more techniques in electrochemistry.

Based on the data for the reference electrode performance, these simplified reference electrodes utilizing the mullite membranes to maintain electrical contact with the melt are sufficient. They combine good qualities such as mechanical strength, ease of construction, inexpensive off-the-shelf materials and reproducibility. Future work can focus on full qualification of these reference electrodes using improved methods as progress has been slowed due to equipment issues.

Molten salt electrochemical techniques need to be improved for use in extraction. The preliminary data show that some experience is required for the use of molten salt electrochemistry but the results here are encouraging. The use of tungsten as a surface for deposition seems appropriate due to its corrosion resistance in these chloride salts. Mill tailings provide an excellent opportunity to study separations as there are many different constituents that are visible in the mixture, electrochemically.

References

1. Ogawa, T.; Minato, K.; Okamoto, Y.; Nishihara, K., Nuclear energy and waste management -- pyroprocess for system symbiosis. *Journal of Nuclear Materials* **2007**, *360*, 12-15.
2. Tahraoui, A.; Morris, J. A., Decomposition of Solvent Extraction Media during Nuclear Reprocessing: Literature Review. *Sep. Sci. Technol.* **1995**, *30* (13), 2603-2630.
3. Mamantov, G.; Hussey, C. L.; Marassi, R., An Introduction to Electrochemistry in Molten Salts. In *Techniques for Characterization of Electrodes and Electrochemical Processes*, Varma, R.; Selman, J. R., Eds. John Wiley & Sons, Inc.: New York, 1991; pp 471-513.
4. Bard, A. J.; Faulkner, L. R., *Electrochemical Methods: fundamentals and applications*. 2nd. ed.; John Wiley & Sons, Inc.: New York, 2001.
5. Liliendahl, W. C.; Driggs, F. H. Uranium, Method of producing rare metals by electrolysis. 1932.
6. (a) Kolodney, M., LA-147 Production of Uranium by Electrolysis of Fused Salts. Los Alamos, NM, 1944; (b) Marsano, C.; Noland, R. A., ANL-5102 The Electrolytic Refining of Uranium. Commission, U. S. A. E., Ed. The University of Chicago, Metallurgy Division: Lemont, IL, 1953.
7. Wilhelm, H. A.; Carlson, O. N., *Transactions of the American Society for Metals* **1950**, *42*, 1311.
8. Lichtenberger, H. V., The Experimental Breeder Reactor. In *Nuclear Engineering, Part III*, The American Institute of Chemical Engineers: New York, 1954; Vol. 50, pp 139-146.
9. Fields, P. R.; Isaac, N. M. Separation of Americium and Curium. 3022134, 02/20/1960, 1960.
10. Moore, F. L.; Mullins, W. T., Separation of Berkelium from Other Elements. Application to Purification and Radiochemical Determination of Berkelium. *Anal. Chem.* **1965**, *37* (6), 687-689.

11. Mullins, L. J.; Beaumont, A. J.; Leary, J. A., Distribution of americium between liquid plutonium and a fused salt. Evidence for divalent americium. *Journal of Inorganic and Nuclear Chemistry* **1968**, *30* (1), 147-156.
12. Leary, J. A.; Mullins, L. J., On divalent americium in molten salt + molten plutonium systems. *The Journal of Chemical Thermodynamics* **1974**, *6* (1), 103-104.
13. Motta, E. E., High-Temperature Fuel Processing Methods. In *Progress in Nuclear Energy*, Bruce, F. R.; Fletcher, J. M.; Hyman, H. H.; Katz, J. J., Eds. McGraw-Hill Book Co., Inc.: New York, 1956; pp 309-315.
14. Niedrach, L. W.; Glamm, A. C., Electrorefining for Removing Fission Products from Uranium Fuels. *Ind. Eng. Chem.* **1956**, *48* (6), 977-981.
15. Niedrach, L. W.; Glamm, A. C., Uranium purification by electrorefining. *Journal of the Electrochemical Society* **1956**, *103* (9), 521-528.
16. *Symposium on the reprocessing of irradiated fuels : discussions, held at Brussels, Belgium, May 20-25, 1957.* Centre d'etudes pour les applications de l'energie nucleaire: Bruxelles, 1957; p 127,27p.
17. Murbach, E. W.; Hansen, W. N., Pyroprocessing Thorium Fuels. *Ind. Eng. Chem.* **1959**, *51* (2), 177-178.
18. Campbell, D. O.; Cathers, G. I., Processing of Molten Salt Power Reactor Fuels. *Ind. Eng. Chem.* **1960**, *52* (1), 41-44.
19. Mullins, L. J.; Leary, J. A.; Morgan, A. N.; Maraman, W. J., LA-2666 Plutonium Electrorefining. Los Alamos, NM, 1962.
20. Mullins, L. J.; Leary, J. A.; Morgan, A. N.; Maraman, W. J., Plutonium Electrorefining. *Ind. Eng. Chem. Proc. Des. Dev.* **1963**, *2* (1), 20-24.

21. Mullins, L. J.; Leary, J. A., LA-3118 Fused Salt Electrorefining of Molten Plutonium and its Alloys. 1964.
22. Christensen, E. L.; Maraman, W. J., LA-3542 Plutonium Processing at the Los Alamos Scientific Laboratory. In *Los Alamos Scientific Laboratory, University of California Report*, 1968.
23. Curtis, M. H.; Hopkins, H. H., Continuous Electrowinning of Plutonium from Chloride Melts. *Electrochemical Technology* **1964**, *2*, 239.
24. Heising, C. D., *The reprocessing decision : a study in policy-making under uncertainty*. Garland Pub.: New York, 1979; p ca. 250 p. in various pagings.
25. Smith, D. H.; McDuffie, H. F., ORNL-TM-6764 A Literature review of selected methods of molten salt reprocessing of ceramic fuels. 1979.
26. Navratil, J. D.; Thompson, G. H., Removal of actinides from selected nuclear fuel reprocessing wastes. *Nucl. Technol.* **1979**.
27. Ragheb, M. M. H., *Nuclear performance of molten salt fusion-fission symbiotic systems for catalyzed DO and DT reactors*. [Dept. of Energy for sale by the National Technical Information Service: Oak Ridge, Tenn. Springfield, Va., 1979; p iii, 39 p.
28. Sakamura, Y.; Hijikata, T.; Kinoshita, K.; Inoue, T.; Storvick, T. S.; Krueger, C. L.; Grantham, L. F.; Fusselman, S. P.; Grimmitt, D. L.; Roy, J. J., Separation of actinides from rare earth elements by electrorefining in LiCl-KCl eutectic salt. *Journal of Nuclear Science and Technology* **1998**, *35* (1), 49-59.
29. Sakamura, Y.; Hijikata, T.; Kinoshita, K.; Inoue, T.; Storvick, T. S.; Krueger, C. L.; Roy, J. J.; Grimmitt, D. L.; Fusselman, S. P.; Gay, R. L., Measurement of standard potentials of actinides (U,Np,Pu,Am) in LiCl-KCl eutectic salt and separation of actinides from rare earths by electrorefining. *Journal of Alloys and Compounds* **1998**, 271-273, 592-596.

30. Kinoshita, K.; Inoue, T.; Fusselman, S. P.; Grimmett, D. L.; Roy, J. J.; Gay, R. L.; Krueger, C. L.; Nabelek, C. R.; Storvick, T. S., Separation of uranium and transuranic elements from rare earth elements by means of multistage extraction in LiCl-KCl/ Bi system. *Journal of Nuclear Science and Technology* **1999**, *36* (2), 189-197.
31. Kinoshita, K.; Inoue, T.; Fusselman, S. P.; Grimmett, D. L.; Krueger, C. L.; Storvick, T. S., Electrodeposition of Uranium and Transuranic Elements onto Solid Cathode in LiCl–KCl/Cd System for Pyrometallurgical Partitioning. *Journal of Nuclear Science and Technology* **2003**, *40* (7), 524-530.
32. Li, S. X.; Johnson, T. A.; Westphal, B. R.; Goff, K. M.; Benedict, R. W. In *Electrorefining Experience for Pyrochemical Processing of Spent EBR-II Driver Fuel*, GLOBAL 2005, Tsukuba, Japan, Tsukuba, Japan, 2005.
33. Castrillejo, Y.; Bermejo, R.; Martinez, A. M.; Barrado, E.; Diaz Arocas, P., Application of Electrochemical Techniques in Pyrochemical Processes -- Electrochemical Behaviour of Rare Earths at W, Cd, Bi and Al Electrodes. *Journal of Nuclear Materials* **2007**, *360*, 32-42.
34. Masset, P.; Apostolidis, C.; Konings, R. J. M.; Malmbeck, R.; Rebizant, J.; Serp, J.; Glatz, J.-P., Electrochemical behaviour of neptunium in the molten LiCl-KCl eutectic. *Journal of Electroanalytical Chemistry* **2007**, *603* (2), 166-174.
35. Kuznetsov, S. A.; Gaune-Escard, M., Electrochemical transient techniques for study of the electrochemistry and thermodynamics of nuclear materials in molten salts. *Journal of Nuclear Materials* **2009**, *389* (1), 108-114.
36. Shriver, D. F.; Drezdson, M. A., *The Manipulation of Air - Sensitive Compounds*. 2nd ed.; John Wiley & Sons, Inc.: Toronto, 1986.
37. AGS-G001 Guidelines for Gloveboxes. American Glovebox Society: 2007.
38. Bockris, J. O. M.; Hills, G. J.; Inman, D.; Young, L., An all -glass reference electrode for molten salt systems. *J. Sci. Instr.* **1956**, *33*, 438-439.

39. Schwarz, E., Porous glass as a substitute for Vycor. Particle Solutions, L., Ed. Alachua, FL, 2010.
40. Davies, K.; Li, S., INL/CON-07-12259 Simplified reference electrode for electrorefining of spent fuel in high temperature molten salt. **2007**.
41. Davies, K., Schwarz, E., Ed. 2010.
42. Danner, G.; Rey, M., *Electrochim. Acta* **1961**, *4*, 274.
43. Erdoes, E.; Altorfer, H., *Electrochim. Acta* **1975**, *20*, 937.
44. Guthrie, J. M. Overview of X-ray Fluorescence.
http://archaeometry.missouri.edu/xrf_overview.html (accessed Apr. 17, 2011).
45. *CRC Handbook of Chemistry and Physics*. 91st ed.; CRC Press: Boca Raton, FL, 2010-2011.

Appendix: Laboratory Molten Salt Procedures

The following are Standard Operating Procedures written for the performance of molten salt chemistry in the laboratory. This is provided as a foundation for future work.